MASTER

EXTERNAL TRANSMITTAL AUTHORIZED
Distribution Limited to Recipients Indicated

ORNL
Central Files Number
60-4-37

135

CHEMICAL TECHNOLOGY DIVISION

UNIT OPERATIONS SECTION

MONTHLY PROGRESS REPORT

APRIL 1960

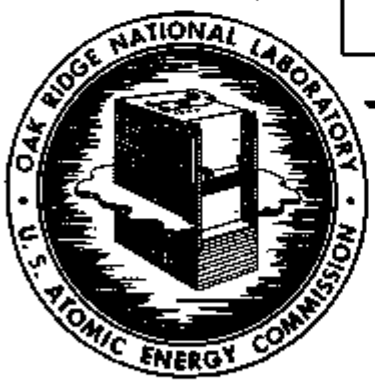

OAK RIDGE NATIONAL LABORATORY
operated by
UNION CARBIDE CORPORATION
for the
U.S. ATOMIC ENERGY COMMISSION

264 - 01

DISCLAIMER

ORNL CF 60-4-37

UNIT OPERATIONS SECTION MONTHLY PROGRESS REPORT

April 1960

CHEMICAL TECHNOLOGY DIVISION

M. E. Whatley
P. A. Haas
R. W. Horton
A. D. Ryon
J. C. Suddath
C. D. Watson

Date Issued

JUL 28 1960

OAK RIDGE NATIONAL LABORATORY
Oak Ridge, Tennessee
Operated By
UNION CARBIDE CORPORATION
for the
U. S. Atomic Energy Commission

ABSTRACT

It has been experimentally verified that 30% tributyl phosphate will not extract acid deficient species of uranyl nitrate. Flooding throughputs for the Mark I stacked clone contactor ranged from 600 cc/min organic at zero aqueous to 60 cc/min organic at 1950 cc aqueous. A large electronic vibrator of 5000 lb thrust was found somewhat inferior to pneumatic vibration for compacting oxide fuels into stainless steel tubes. Tests were started on the use of fixed bed CuO oxidizers for removing hydrogen contamination from helium gas streams. None of the variables studied within this period effected an increase in particle size in the denitration of thorium nitrate to produce ThO_2. The rate of uranyl sulfate loading on nitrate equilibrated Dowex 21K appears to be essentially independent of the loading solution sulfate concentration. The nitric acid concentrations corresponding to maximum UO_2-ThO_2 pellet dissolution rate were 15.5 M for Thorex solution and 13 M for the adjusted Darex solution. Two additional semi-continuous Sulfex declad and Thorex core dissolutions of prototype Consolidated Edison fuel assemblies were made to complete the series of runs. The effective area of cylindrical UO_2 pellets dissolving in nitric acid was estimated from experimental rate measurements as a function of the fraction dissolved. A prototype SRE fuel rod was hydraulically expanded about 45 mils at 1300 psig pressure. Flooding capacities have been determined for the compound extraction scrub columns with the acid Thorex flowsheet. A controlled cold bath has been installed for the condensation pressure analyzer to be used for UF_6 stream analysis. Tracer studies with the 8-in. dia x 84-in. high waste calcination vessel showed the solid deposition pattern to be partly a radial growth from the side wall and partly a vertical growth from the bottom.

CONTENTS

Previous Reports in This Series for the Years 1959-1960

January	ORNL CF 59-1-74
February	ORNL CF 59-2-45
March	ORNL CF 59-3-61
April	ORNL CF 59-4-47
May	ORNL CF 59-5-47
June	ORNL CF 59-6-63
July	ORNL CF 59-7-58
August	ORNL CF 59-8-76
September	ORNL CF 59-9-69
October	ORNL CF 59-10-77
November	ORNL CF 59-11-54
December	ORNL CF 59-12-49
January	ORNL CF 60-1-49
February	ORNL CF 60-2-56
March	ORNL CF 60-3-61

All previous reports in this series are listed in the June 1959 report, CF 59-6-63, from the beginning, December 1954.

SUMMARY

1.0 CHEMICAL ENGINEERING RESEARCH

Distribution coefficients have been measured for acid deficient uranyl nitrate between water and 30% TBP in Amsco. Measurements of pH of the aqueous phases before and after extraction and stripping showed that only neutral (stoichiometric) uranyl nitrate was extracted. Feed solutions of from 550 g U/liter to 30 g per liter from 0 to 0.3 mols acid deficient/mol U were used.

2.0 FISSION PRODUCT RECOVERY BY SOLVENT EXTRACTION

Holdup, flooding, and organic entrainment data for Mk I stacked clone contactor with the system Amsco - 0.08 M HNO_3 show total holdups of 50 to 274 cc for five clone stages and de-entrainer over aqueous rates of 82 to 1950 cc. Flooding throughputs with Amsco range from 600 cc/min organic at zero aqueous to 60 cc/min organic at 1980 cc aqueous.

3.0 FUEL CYCLE DEVELOPMENT

Eleven runs made with an impact, air driven piston type vibrator gave ThO_2-3.4 wt % UO_2 densities of 8.5 to 8.9 g/cc in 2 ft length of 3/8-in. o.d. stainless steel tubes. Use of narrow size fractions or careful premixing of the fractions prior to loading the tubes does not appear to be as important to obtaining high compacted densities as originally indicated. Use of a large electronic vibrator of 5000 lb thrust gave densities of 8.23 to 8.51 g/cc or 8.38 g/cc average while additional pneumatic vibration of the same tubes give densities of 8.50 to 8.75 g/cc or 8.63 g/cc average.

4.0 GCR COOLANT CLEAN-UP STUDIES

Test of the fixed bed CuO oxidizer was started, using a hydrogen contaminated helium gas stream for the initial test gas. The oxidation of the hydrogen by the CuO was 96.0 to 99.5% complete at a bed temperature of approximately 440°C and bed depth of 1/4 to 1/2 inch.

5.0 HR THORIUM BLANKET STUDIES

Examination of variables which might effect an increase in the flame denitration product particle size from the previously obtained 1 to 2μ to the desired 5 to 10μ dia has continued. None of the variables within the range studied shows promise of yielding this increase. Use of H_2O in place of CH_3OH as the feed solvent or of N_2 in place of O_2-C_3H_8 as the atomizing gas shows no effect. The average dia increases from within 1.0 to 1.6μ at 1500°C to within 1.4 to 2.0μ at 900°C.

6.0 ION EXCHANGE

The rate of uranyl sulfate loading on nitrate equilibrated Dowex 21K appears to be essentially independent of the loading solution sulfate concentration and corresponds to an apparent uranium diffusion coefficient of 1.6×10^{-7} sq cm/sec. This lack of dependence on sulfate concentration is probably

due to the relatively high mobility of the sulfate ion. Nitrate elution of 1200μ Dowex 21K gave an apparent uranium diffusion coefficient of approximately 2×10^{-7} sq cm/sec, and chloride elution gave an apparent coefficient of approximately 4×10^{-7} sq cm/sec.

7.0 POWER REACTOR FUEL PROCESSING

Darex-Thorex

Using a dissolution technique for UO_2-ThO_2 pellets wherein a batch of dissolvent is continuously recirculated between a refluxing dissolver and a well-mixed external reservoir, dissolvents containing 13-15 M HNO_3, 0.04 M F and 53 g SS/liter gave average dissolution rates from 8-45% higher than the Thorex counterparts containing 0.1 M Al in place of the dissolved stainless steel. With the SS dissolvent 13 M HNO_3 produced the higher rate while in the Thorex solution the higher HNO_3 (15.5 M) produced the higher rate.

Sulfex

Two additional semi-continuous Sulfex declad and Thorex core dissolution of prototype Consolidated Edison fuel assemblies were made which completes the series of runs that were made for the purpose of determining reaction rates, dissolution rates, declad time, product loading, cross contaminations of the clad and core dissolvents and its effect on passivation, and thorium and uranium losses to the declad solution. Additional data resulting from these runs show that:

a. thorium losses to the declad solution in the presence of a heel was 0.2% as compared to 0.08% in the absence of a heel,

b. neither boron or sodium are lost by volatilization or precipitate during core dissolution,

c. based on the results of one run, dissolution of the clad started immediately when the declad dissolvent was "spiked" with 0.1 M HCOOH,

d. the semi-continuous core dissolutions plus a 23 hr batch dissolution of the heel (3.6% of UO_2-ThO_2 charged to dissolver) resulted in 99.98% dissolution of UO_2-ThO_2 pellets charged.

Mechanical Processing - Leaching

The effective area of cylindrical UO_2 pellets dissolving in nitric acid was estimated for experimental rate measurements as a function of the fraction dissolved. The results can be approximated by the equation:

$$\frac{A_p}{A_o} = 1 + 47x^2 - 92x^3 + 44x^4$$

where A_o = area of initial cylinder (D/L ~ 1)

A_p = effective area of porous, partially dissolved pellet

x = fraction dissolved, by weight.

SRE Dejacketing Studies

Initial operability tests were successful on the equipment for dejacketing the SRE, NaK bonded, stainless steel clad uranium fuel rods. A prototype fuel rod was hydraulically expanded ~45 mils at 1300 psig pressure.

8.0 SOLVENT EXTRACTION STUDIES

Work was started to evaluate the flow capacity and stage efficiency of pulse columns as a function of operating variables and cartridge design for the acid Thorex flowsheet. Maximum capacity for a compound extraction scrub column with sieve plate cartridges (0.125-in.-dia holes, 23% free area) was 1030 GSFH for aqueous-continuous operation and 1690 GSFH for organic-continuous operation. Maximum capacity in the compound extraction scrub column with a nozzle plate cartridge (0.125-in.-dia holes, 10% free area) was 1400 GSFH. Maximum capacity for stripping columns operated organic continuous was 1290 GSFH for sieve plate cartridges and 2280 GSFH for nozzle plate cartridges (0.188-in.-dia holes, 23% free area). For aqueous-continuous operation, it was 1290 GSFH for sieve plate cartridge and 2080 GSFH for the nozzle plate cartridge.

9.0 VOLATILITY

UF_6 Stream Analysis

A CPA (condensation pressure analyzer) has been installed for test. Accurate analysis requires that the capillary in which condensation occurs be held at a constant temperature. A cold bath controlled by the volume change due to freezing a liquid maintained a temperature of 0°C ± 0.001°C with H_2O and -22.8°C ± 0.2°C with CCl_4 as the liquids.

Moving Bed Absorber Test

The effect of loading the NaF bed with HF was investigated. Discharge pressure increased from 40 to 140 psig. The sorption pattern in the bed was determined by a thermocouple array.

10.0 WASTE PROCESSING

In an 8-in. dia by 84-in. high vessel, synthetic Purex waste to which calcium hydroxide had been added was evaporated and calcined at an average feed rate of 16 liters/hr. Injections of Cr-51 and Nb-95 tracers in the feed stream showed the solid deposition pattern to be partly a radial growth from the side wall and partly a vertical growth from the bottom.

Equipment development was begun relative to the remote connection, disconnection and removal of calciner vessels in a pilot plant for high level wastes. A tool consisting of a long-handled socket wrench which rotates to the bolt positions was developed for attaching and removing flanges remotely.

An air stream bearing $Cr(NO_3)_3$ aerosols containing Cr-51 tracer was completely decontaminated by passage through a 3-in. dia packed distillation tower 10 ft high over a range of vapor compositions of 0.30 to 0.95 mol fraction steam. In the absence of the steam in the vapor phase decontamination factors below 10 were measured.

1.0 CHEMICAL ENGINEERING RESEARCH

A. D. Ryon

1.1 Extraction of Acid Deficient Uranyl Nitrate by 30% TBP in Amsco - C. V. Chester

Information on the nature of the extracting species in acid deficient uranyl nitrate solutions was desired and, in particular, if an acid deficient species could be extracted.

pH Measurement. Since uranyl ion hydrolyzes, a convenient method of following the acid deficiency of a solution is by pH measurement. Acid deficient solutions of uranyl nitrate were prepared by dissolving UO_3 in either neutral uranyl nitrate solution (series 0, 1, and 2) or in nitric acid (series U-0, U-1, U-2, and U-3). The neutral uranyl nitrate was prepared by careful recrystallization from water. The pH of solutions so made up is plotted against concentration in Figure 1.1. Acid deficiency is reported per mol of uranium, rather then per liter of solution, as the solutions of a series were prepared simply by diluting a concentrated stock solution. A cross plot of pH against nominal acid deficiency is shown in Figure 1.2. The solutions 0.156 and 0.200 mol acid deficient/mol U do not have pH's consistent with the other solutions. In the case of the 0.156 solution, it is probably an error in making up the solution. In the case of 0.200, there may have been enough U_3O_8 in the UO_3 to account for the difference. These curves will be checked using a superior neutral uranyl nitrate prepared by vacuum desiccation.

Extraction Studies. The aqueous solutions so prepared were extracted by an equal volume of 30% TBP in Amsco. The feed, raffinate, and extract were analyzed for uranium potentiometrically. The pH of the feed and raffinate were measured on a Beckman pH meter. The data are presented in Table 1.1 for series 0, 1, and 2. The pH relations of the feed and raffinate are shown graphically in Figures 1.3, 1.4, and 1.5. The raffinate is usually more acid deficient than the feed, indicating that the acid deficient species is less extractable. The exception is series 0, where the raffinate is more acid than the extract. It is felt that this is a spurious result, possibly caused by solution decomposition.

1.2 Extraction and Stripping Studies

In series U, solutions were made up by dissolving UO_3 in nitric acid solutions prepared from 15.75 N reagent grade HNO_3. The stock solutions were used to prepare a series of dilutions used for the feed solutions. The feed was extracted with an equal volume of 30% TBP, and then the organic was stripped with an equal volume of distilled water. All phases were sampled for potentiometric uranium analysis, and pH of the aqueous phase was measured at each step. The data are presented in Table 1.2. The pH relations of the feed, raffinate, and strip solutions are shown in Figures 1.6, 1.7, 1.8, and 1.9. Series U-0, shown in Figure 1.6, was intended to be neutral. It turned out to be slightly acid, indicating a slight error in weighing, or more likely, in pipetting. The relation of the feed, raffinate, and strip,

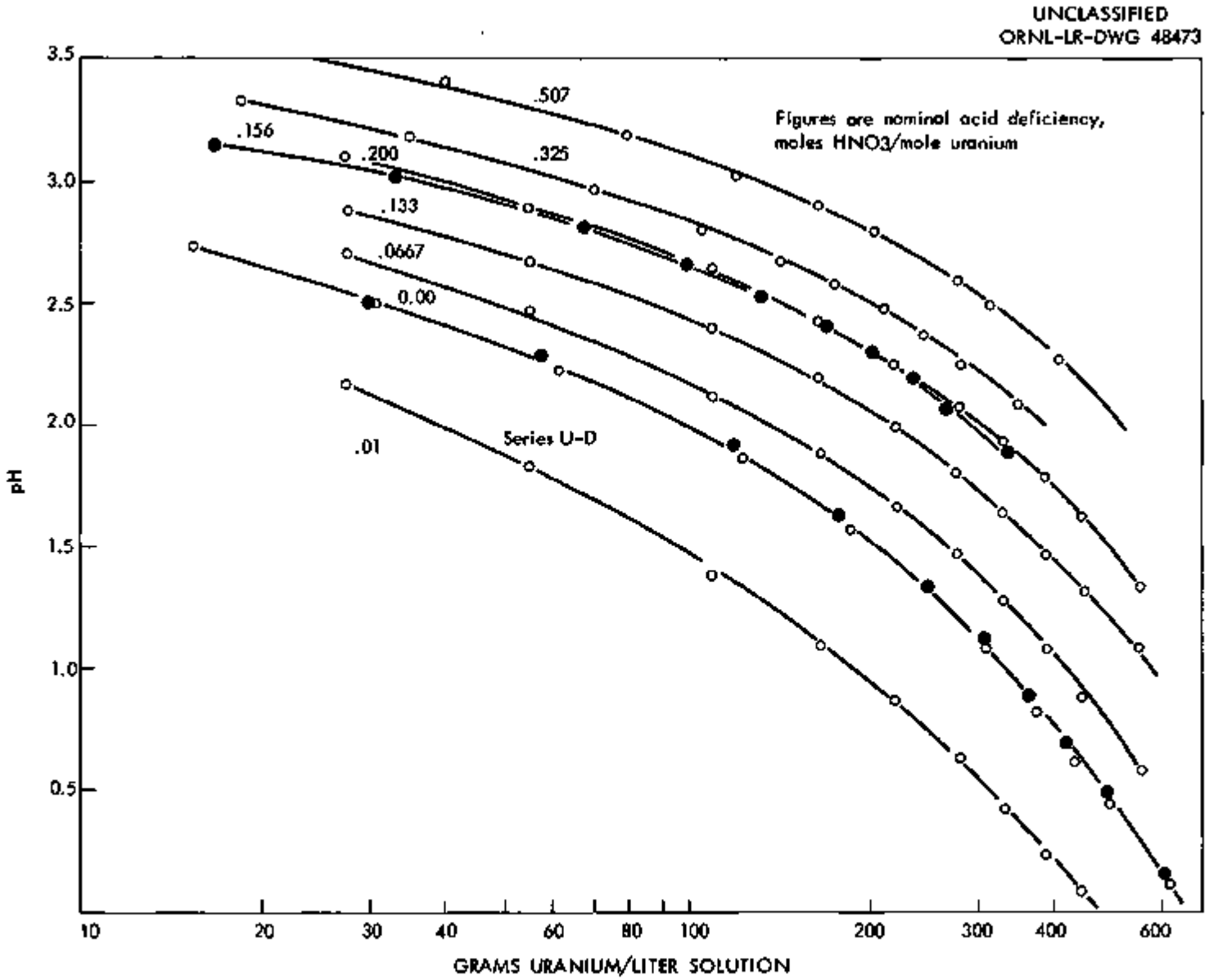

Fig. 1.1. pH of uranyl nitrate solutions in acid deficient region.

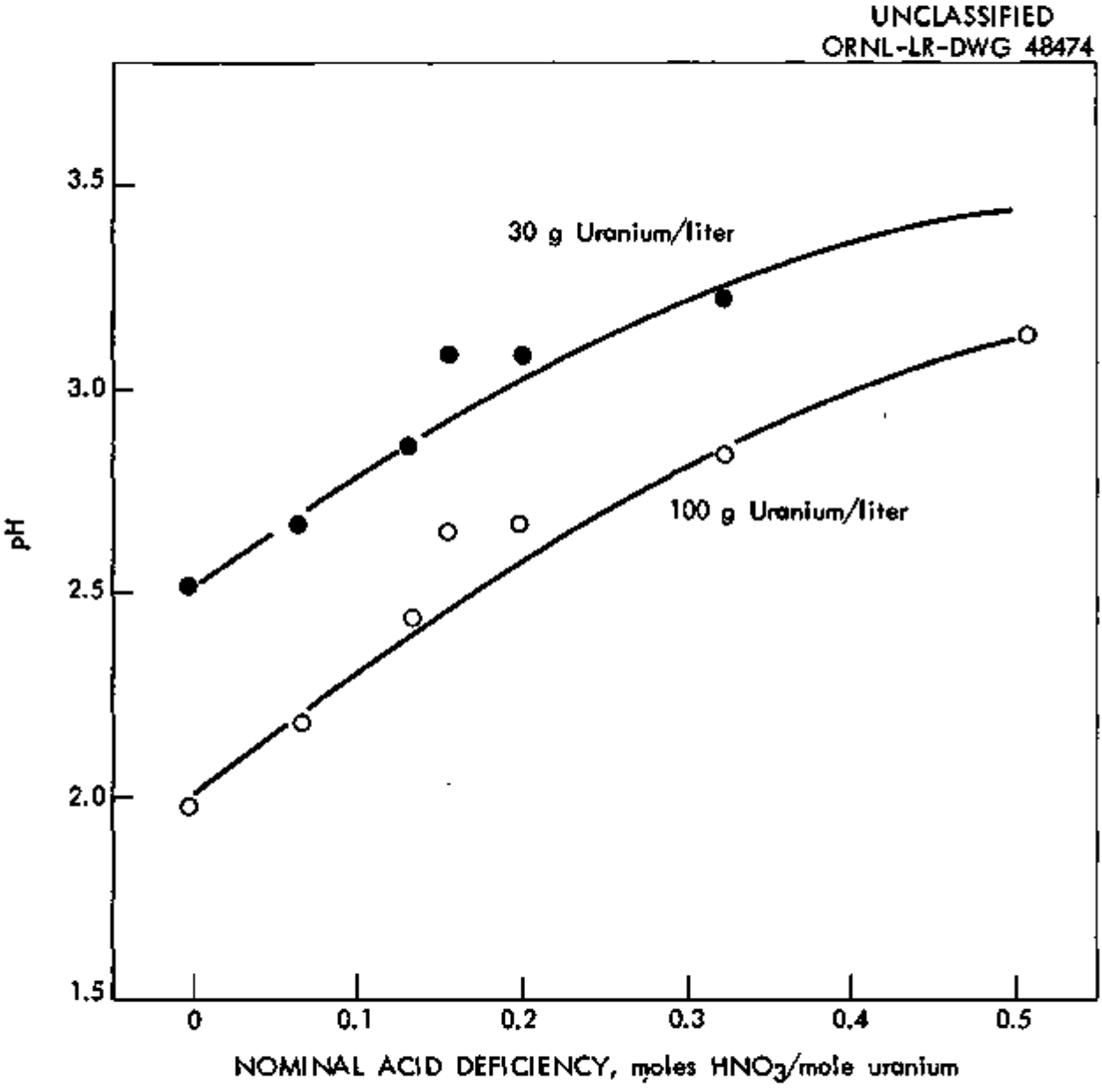

Fig. 1.2. pH vs nominal acid deficiency for uranyl nitrate solutions.

Table 1.1. 1-stage Extraction of Acid Deficient Uranyl Nitrate by 30% in Amsco

Run	Feed		Raffinate		Extract,
	g/liter	pH	g/liter	pH	g/liter
Series 0. Nominally neutral.					
0-10	612.18	0.15	490.1	0.45	122.3
0-8	496.1	0.48	374.5	0.88	118.3
0-7	422.58	0.70	308.3	1.09	116.9
0-6	362.78	0.90	253.3	1.32	116.5
0-5	304.59	1.12	196.2	1.52	109.6
0-4	250.24	1.38	143.2	1.71	98.37
0-3	179.20	1.64	97.76	1.91	82.57
0-2	120.32	1.92	61.06	2.04	58.03
0-1	58.80	2.29	32.25	2.26	25.14
0-0.5	30.33	2.58	20.26	2.49	7.75
Series 1. Nominally 0.325 mols acid deficient/mol U.					
1-10	356	2.10	252.2	2.50	109.3
1-8	284.8	2.24	187.4	2.72	98.98
1-7	248.6	2.36	159.3	2.80	90.89
1-6	210.8	2.47	137.7	2.89	80.43
1-5	175.8	2.57	108.6	2.99	69.43
1-4	143.4	2.66	85.71	3.10	57.15
1-3	107.1	2.79	65.14	3.18	41.13
1-2	70.83	2.95	45.66	3.25	25.65
1-1	35.17	3.18	25.97	3.30	9.34
1-0.5	18.57	3.31	15.37	3.37	2.75
Series 2. Nominally 0.156 mols acid deficient/mol U.					
2-10	336	1.84	227.9	2.32	112.8
2-8	268.5	2.05	169.3	2.54	100.4
2-7	235.6	2.19	141.5	2.62	91.14
2-6	201.6	2.28	124.2	2.73	83.41
2-5	169.2	2.40	94.98	2.82	70.75
2-4	133.6	2.53	75.33	2.96	58.13
2-3	100.1	2.66	57.03	3.02	43.30
2-2	67.56	2.80	40.41	3.08	26.66
2-1	33.06	3.01	23.32	3.18	9.267
2-0.5	16.74	3.15	13.65	3.20	28.01

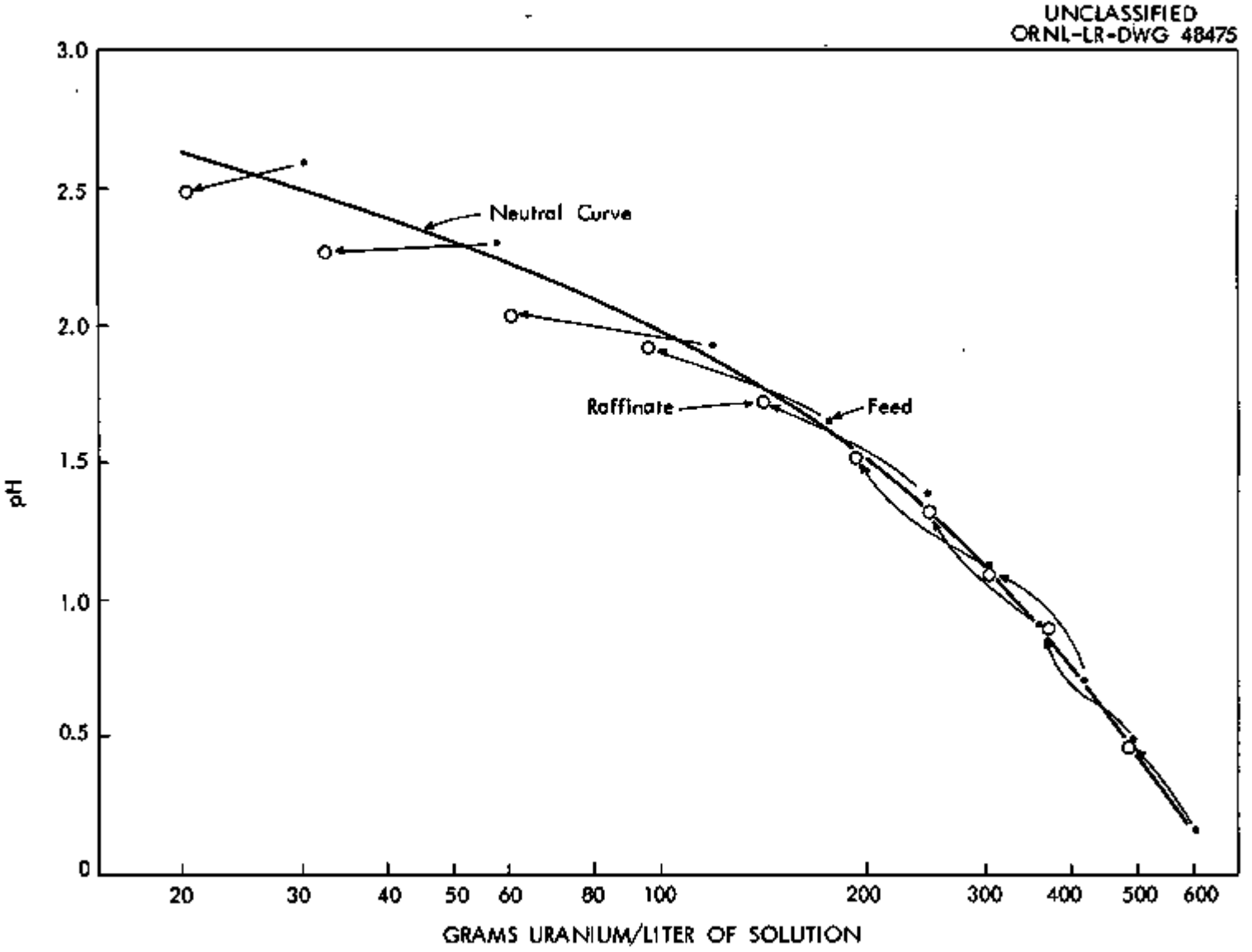

Fig. 1.3. Series O extraction of uranyl nitrate by 30% TBP in Amsco aqueous solution initially nominally neutral.

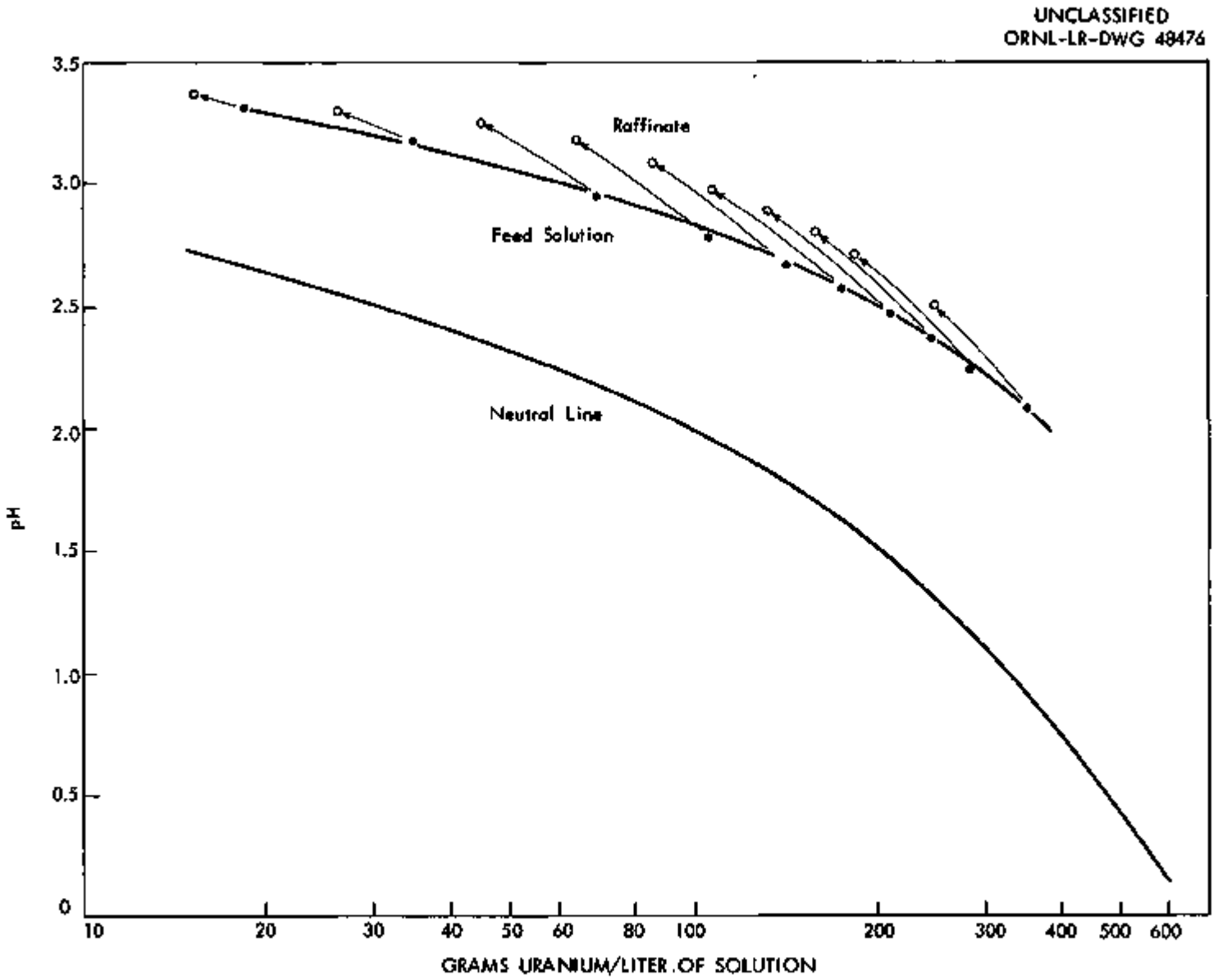

Fig. 1.4. Series 1. Extraction of uranyl nitrate by 30% TBP aqueous initially .325 nominal moles acid deficient per mole uranium.

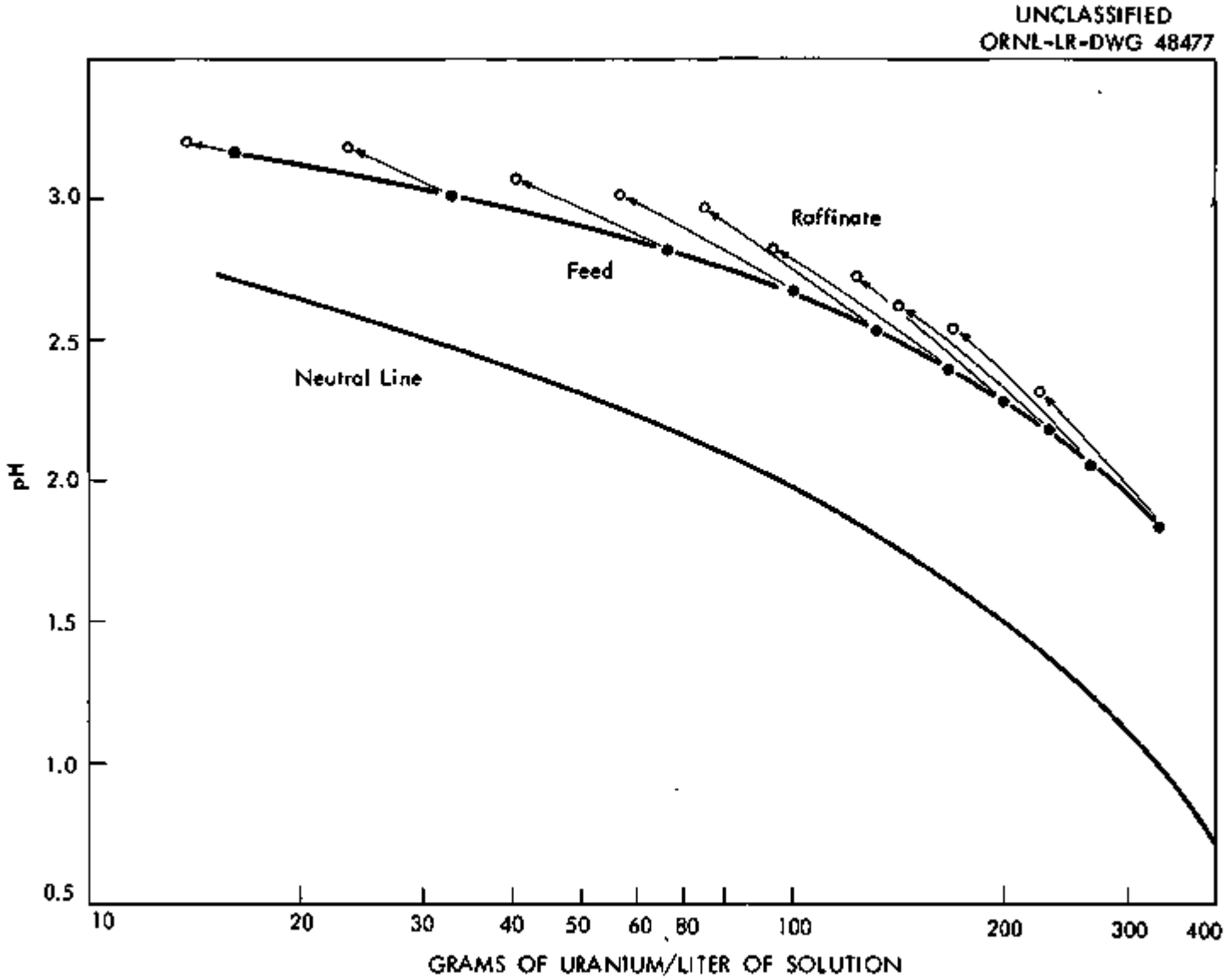

Fig. 1.5. Series 2. Extraction of acid deficient uranyl nitrate by 30% TBP in Amsco. Aqueous solution initially 0.156 nominal mole acid deficient/mole uranium.

Table 1.2. U-Series - 1-stage Extraction and Stripping of Acid Deficient Uranyl Nitrate by 30% TBP in Amsco

Run	Feed,		Extraction			Stripping		
			Raffinate,		Extract,	Strip Solution,		Lean Organic,
	g/ℓ	pH	g/ℓ	pH	g/ℓ	g/ℓ	pH	g/ℓ
Series U-0 - Nominally 0.01 M excess HNO_3/mol uranium								
U-0-10	553.2	0	441.3	0	121.1	62.63	2.09	57.86
U-0-8	446.4	0.08	331.0	0.33	118.3	60.39	2.09	57.10
U-0-7	390.8	0.22	277.2	0.50	115.7	59.21	2.09	56.49
U-0-6	336.5	0.41	222.6	0.71	113.5	57.81	2.10	54.76
U-0-5	284.2	0.63	170.4	0.90	108.0	54.30	2.12	51.04
U-0-4	222.4	0.87	127.11	1.10	96.44	49.19	2.17	46.37
U-0-3	166.4	1.10	87.10	1.32	78.36	41.38	2.22	36.37
U-0-2	110.5	1.38	55.69	1.58	54.18	31.61	2.30	23.71
U-0-1	55.21	1.83	30.45	1.91	24.44	16.95	2.50	6.497
U-0-0.5	27.49	2.17	18.49	2.20	6.50	7.631	2.75	1.180
Series U-1 - Nominally 0.0667 mols acid deficient/mol uranium								
U-1-10	557.4	0.59	447.5	0.98	118.3	62.29	2.05	57.54
U-1-8	447.0	0.88	351.8	1.32	115.7	62.00	1.77	54.03
U-1-7	390.8	1.08	280.3	1.54	114.4	60.73	1.75	53.38
U-1-6	333.2	1.27	224.2	1.75	112.2	57.31	1.85	53.17
U-1-5	279.6	1.47	174.7	1.93	105.0	54.39	1.84	50.44
U-1-4	222.1	1.66	129.9	2.12	92.57	48.96	1.84	44.50
U-1-3	166.5	1.88	90.03	2.35	76.41	40.80	1.84	34.53
U-1-2	112.2	2.11	57.36	2.51	54.13	29.94	1.97	20.23
U-1-1	55.02	2.46	31.63	2.68	21.60	16.40	2.25	4.550
U-1-0.5	27.91	2.70	19.31	2.74	8.944	6.714	2.27	1.052
Series U-1 - Checks of decomposed solutions								
U-1C-10	550.8	0.58	432.2	0.96	119.7	61.70	2.25	58.42
U-1C-6	326.6	1.28	214.2	1.73	110.6	55.77	2.27	53.63
U-1C-5	270.4	1.46	161.6	1.93	100.5	52.66	2.28	49.63
U-1C-4	224.2	1.68	129.9	2.12	93.59	47.16	2.32	42.52
Series U-2 - Nominally 0.133 mols acid deficient/mol uranium								
U-2-10	556.4	1.06	425.4	1.39	119.6	62.24	2.26	57.33
U-2-8	445.5	1.31	331.5	1.73	118.1	59.38	2.27	57.36
U-2-7	392.1	1.45	274.0	1.91	115.7	59.33	2.28	55.49
U-2-6	334.9	1.64	207.8	2.09	111.6	58.97	2.29	54.62
U-2-5	280.9	1.80	176.5	2.28	101.1	54.32	2.31	47.24
U-2-4	227.3	1.97	132.4	2.47	92.56	48.16	2.37	44.72
U-2-3	167.8	2.19	86.25	2.64	74.74	39.97	2.42	33.25
U-2-2	111.6	2.40	56.08	2.81	50.77	29.50	2.53	21.40
U-2-1	56.43	2.66	32.12	2.94	23.78	15.82	2.71	5.307
U-2-0.5	27.21	2.88	19.09	3.02	10.36	7.155	2.91	0.759

continued

Table 1.2 (Continued)

Run	Extraction					Stripping		
	Feed,		Raffinate,		Extract,	Strip Solution,		Lean Organic,
	g/ℓ	pH	g/ℓ	pH	g/ℓ	g/ℓ	pH	g/ℓ
Series U-3 - Nominally 0.200 mols acid deficient/mol uranium								
U-3-10	552.6	1.33	444.4	1.65	118.5	61.82	2.12	56.83
U-3-8	447.1	1.62	326.4	1.98	115.4	59.23	2.12	56.28
U-3-7	388.6	1.78	219.9	2.13	112.4	58.42	2.12	52.00
U-3-6	327.6	1.92	228.2	2.31	108.6	55.28	2.14	52.81
U-3-5	290.6	2.07	176.1	2.51	99.69	51.27	2.19	47.3
U-3-4	220.5	2.25	133.5	2.68	87.36	45.46	2.20	40.87
U-3-3	166.4	2.42	93.70	2.81	66.38	37.07	2.28	31.80
U-3-2	109.9	2.63	62.95	2.98	48.39	27.84	2.39	19.89
U-3-1	54.43	2.88	34.17	3.11	20.10	14.86	2.62	5.58
U-3-0.5	26.88	3.10	20.11	3.17	7.58	6.74	2.86	

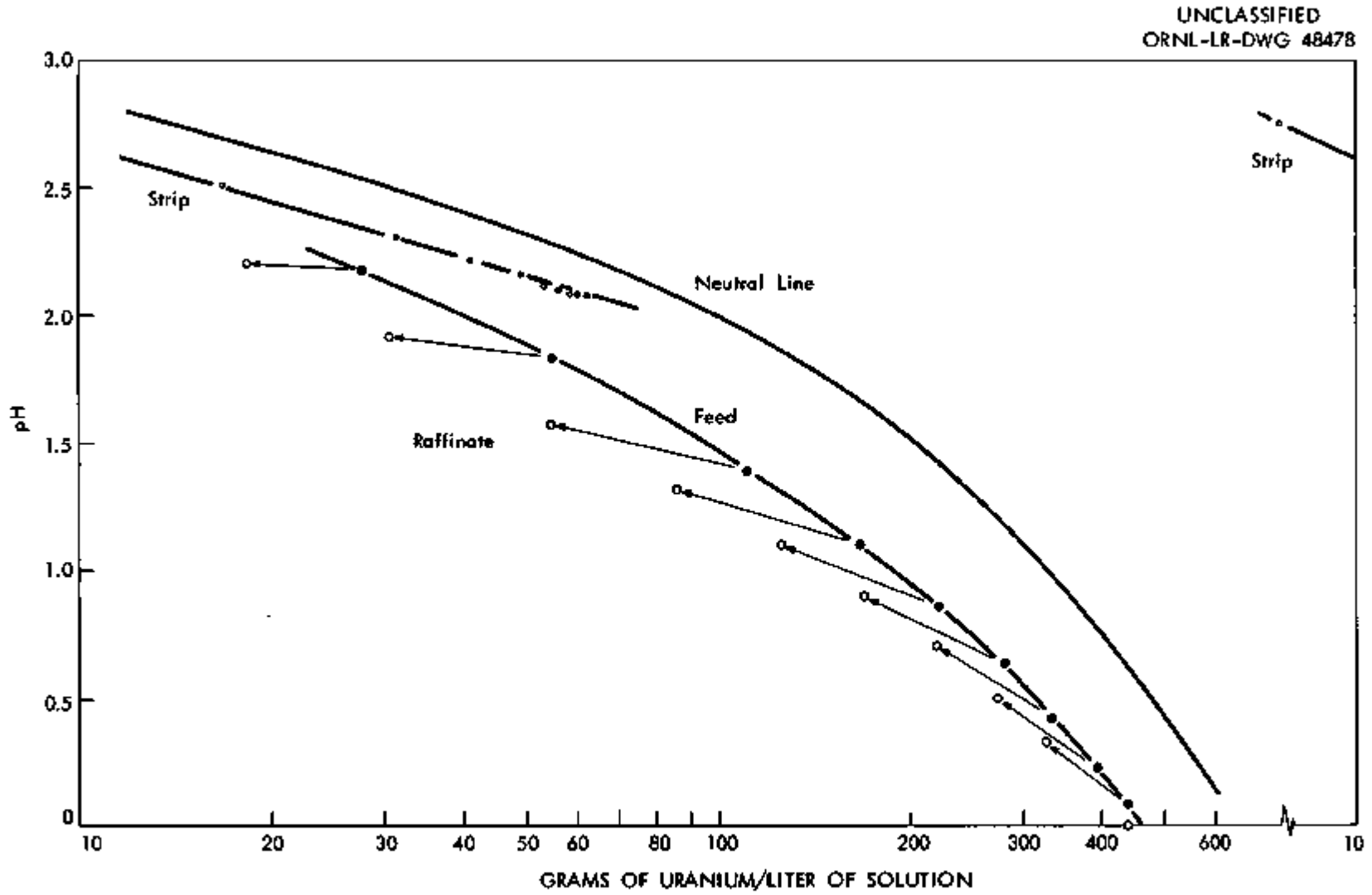

Fig. 1.6. Series U-O. Extraction of slightly acid uranyl nitrate.

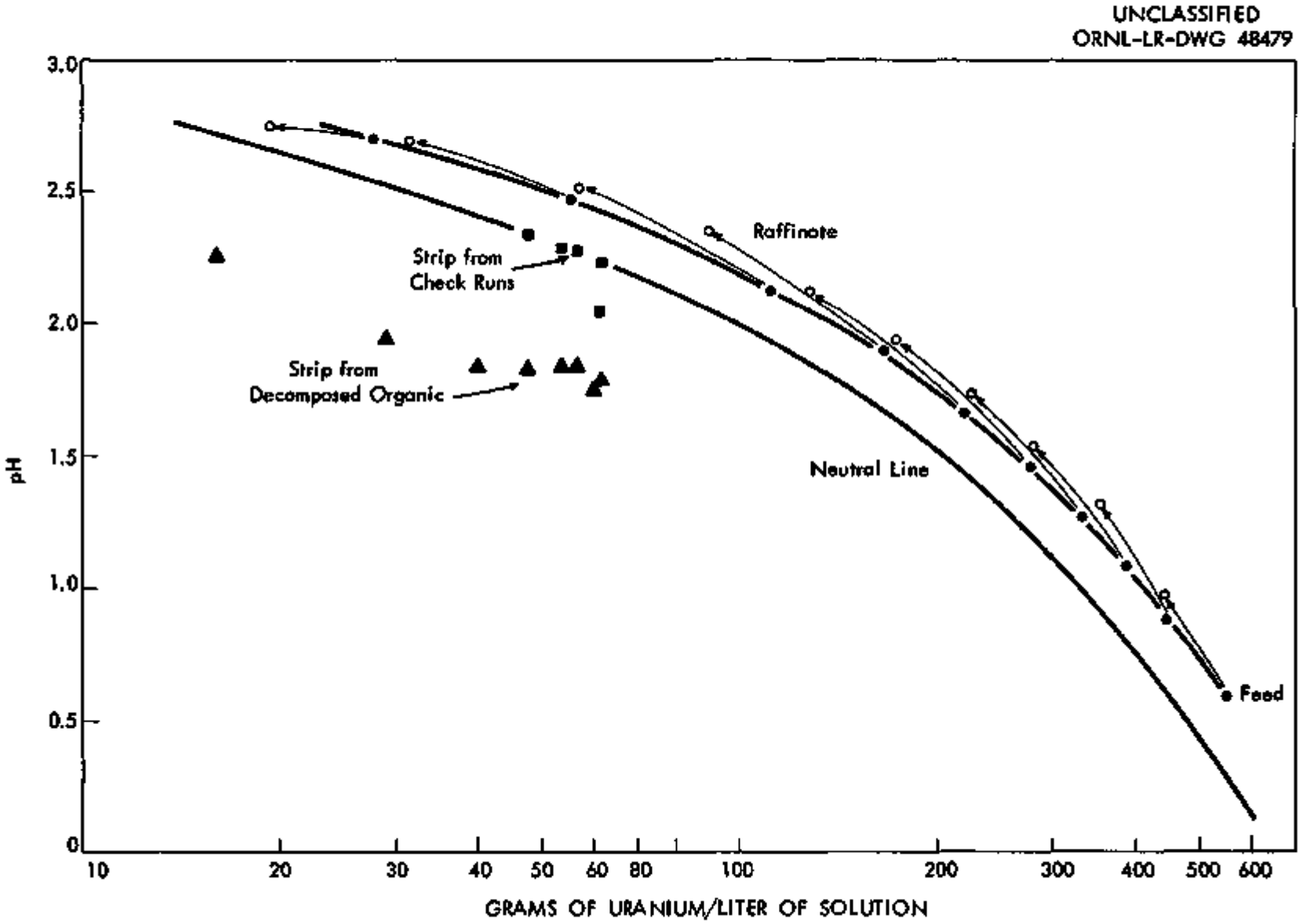

Fig. 1.7. Series U-1. Extraction of 0.067 nominal moles acid deficient per mole of uranium.

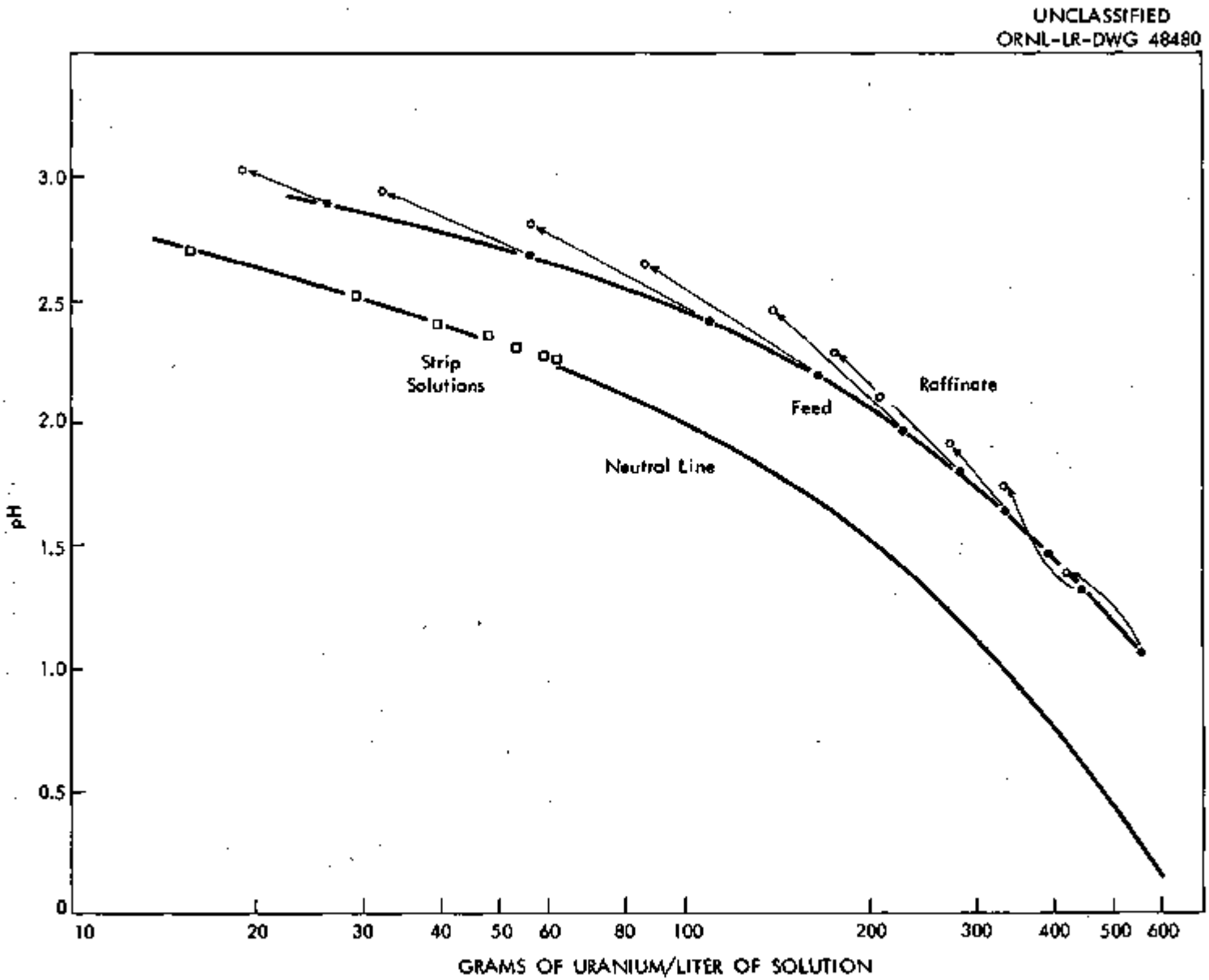

Fig. 1.8. Series U-2. Extraction of 0.133 nominal moles acid deficient per mole of uranium.

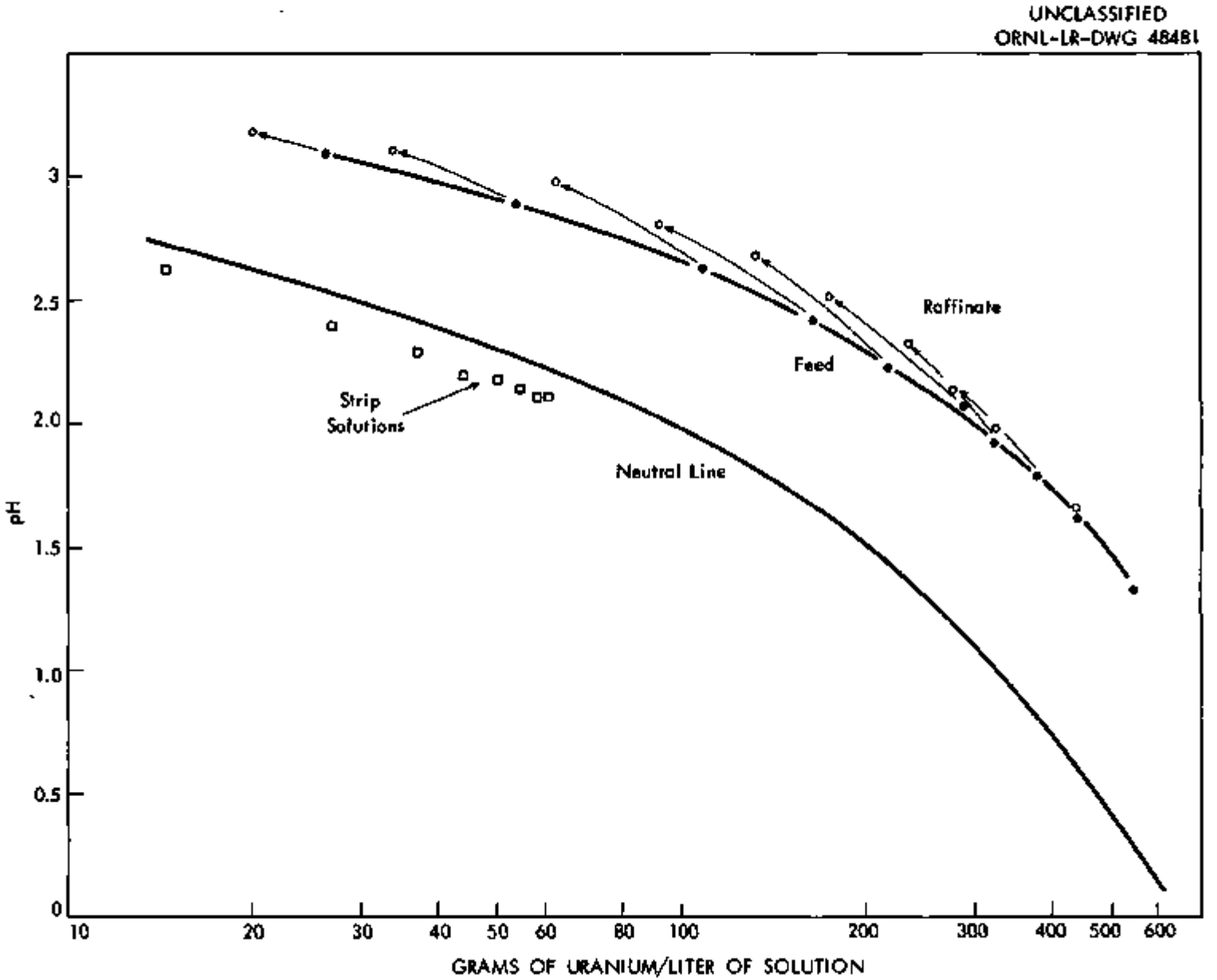

Fig. 1.9. Series U-3. Extraction of 0.200 nominal moles acid deficient/mole uranium.

indicates that uranium is more extractable than acid, and that a little acid extracts, which we already knew. Series U-1, U-2, and U-3 are more interesting; these series were definitely acid deficient. The raffinates were even more acid deficient. However the strip solutions, when prepared quickly, were quite neutral, indicating that the extracted species is the neutral uranyl nitrate.

Upon standing, the organic solutions were observed to slowly darken, turning more orange after a day or so, and precipitating a black solid, presumably U_3O_8, after 1 to 4 days, depending on solution strength and acid deficiency. Series U-1 organic was permitted to stand for two days before stripping, and darkening was observed. This and the scattered pH's indicated decomposition, so 4 of the solutions were re-run, with prompt stripping. The results in Figure 1.7 show clearly the effect of the decomposition of the solutions permitted to stand. The precise neutrality of the checks is also apparent.

Series U-2 was also run quickly, and the strip solutions are quite neutral. In series U-3, the strip solutions are very slightly acid, although the organic was allowed to stand only a few hours. This quite acid deficient solution is very unstable, producing precipitates after only one day.

2.0 FISSION PRODUCT RECOVERY BY SOLVENT EXTRACTION

A. D. Ryon

2.1 Stacked Clone Contactor - W. M. Woods, G. Jones, Jr.

Processing of radioactive fuels by solvent extraction subjects the solvent to radiation damage. Minimizing the contact time of the solvent per theoretical stage would reduce the damage to the solvent. This requires a contactor of high efficiency and low holdup time. The stacked clone contactor has promise of meeting these requirements. The physical design and principle of operation of the stacked clone contactor have been previously reported* together with preliminary evaluations of stage efficiency. The present report presents data on flooding, organic solvent entrainment with the aqueous underflow, and on organic solvent holdup under a wide range of conditions of operations.

2.2 Flooding and Holdup Data

Flooding runs were made using five clone stages and top de-entrainer section. The organic solvent was Amsco. The aqueous feed was 0.08 M HNO_3. Organic feed in most of the runs was to the inlet port of the lowermost clone, i.e., feed was introduced along with the stage recycle stream. A few check runs were made in which the organic feed was introduced into the inlet port of the next stage above the bottom, leaving the bottom stage in place with recycle pump running. The flooding curves ignoring entrainment were identical in these cases.

Flooding points were determined by setting and maintaining an aqueous feed rate with a sequence of increasing organic rates. At each organic rate note was made as to the condition of the contactor, i.e., flooded or not flooded. The organic flow rate at the flooding point was bracketed within 5% of less in this way. Because of the relatively low organic inventory in the stacked clone contactor an incipient flooding condition is quite apparent within a minute or two. However, rates were held constant for at least five minutes, or until a clear-cut flooding condition was seen.

The onset of flooding in the stacked clone contactor took two forms. At aqueous rates below about 1200 cc/min flooding started with an accumulation of solvent in the clone second from the top. The distinct organic vortex surrounded by a much clearer aqueous region observed at operating throughputs was lost, the whole clone being filled with an opaque dispersion. This condition progressed down cascade stage by stage, and finally resulted in gross entrainment of solvent with the aqueous outflow.

At aqueous rates above about 1200 cc/min, flooding began at the organic feed stage (bottom or next to bottom clone) with immediate entrainment of solvent out the underflow port of the feed stage.

---

* Unit Operations Section monthly report, September 1959, CF 59-9-69.

Total solvent holdup of five stages plus top de-entrainer was measured at various aqueous and solvent rate combinations by fixing the organic inlet and aqueous outlet rates and hand-controlling the interface in the top de-entrainer by regulating aqueous input. When the system had stabilized all inlet and outlet streams were shut off, and the total solvent holdup was measured by bringing the interface to its original level, by introducing aqueous feed, the solvent overflowing at the jack-leg being caught and measured.

Figure 2.1 shows the flooding curve and total holdup contours for five stages plus top de-entrainer over the entire range of operable Amsco and 0.08 M HNO_3 flows. As compared to similar data previously reported for the same contactor with Supersol in place of Amsco, flooding occurs at lower throughputs and solvent holdup is somewhat higher at comparable flow rates.

Data are not yet available for separating the individual stage solvent holdups from that of the de-entrainer for the Amsco—0.08 M HNO_3 system. However, data on Supersol and observation of the operating equipment suggests that the holdup is roughly equally divided between the five clone stages with pumps and the top de-entrainer.

Figure 2.2 is a plot of the raw flooding data before correction of the organic flow to account for entrainment of organic with the aqueous. At extreme A/O as well as at high aqueous rates the entrainment of organic with the aqueous represented a significant proportion of the organic input, and correction must be made. Figure 2.1 has been corrected to a throughput basis.

The flooding data for the Supersol—0.08 M HNO_3 system is also plotted on Figure 2.1 and Figure 2.2. Entrainment data on Supersol are not available to allow correction, but it is apparent that the behavior of the two solvents is quite different.

Figure 2.3 is a plot of total organic holdup in five clone stages plus de-entrainer as a function of organic and aqueous throughput. The fact that the lines converge and cross indicates that the holdup is relatively insensitive to aqueous throughput at low organic throughputs. For example, in the region around 75 cc/min organic throughput the holdup varies from 60 cc to 120 cc total over an aqueous throughput range of 0 to 1720 cc/min. This same information has been crossplotted to Figure 2.1 as holdup contours on the flooding data plot.

2.3 Organic Entrainment with Aqueous

The organic entrained with the aqueous was measured by taking 250-ml aqueous samples in volumetric flasks during the course of the holdup runs, allowing these to stand overnight and coalesce, and then "titrating" these with water to bring, first, the organic interface, and then the organic-water interface to the line.

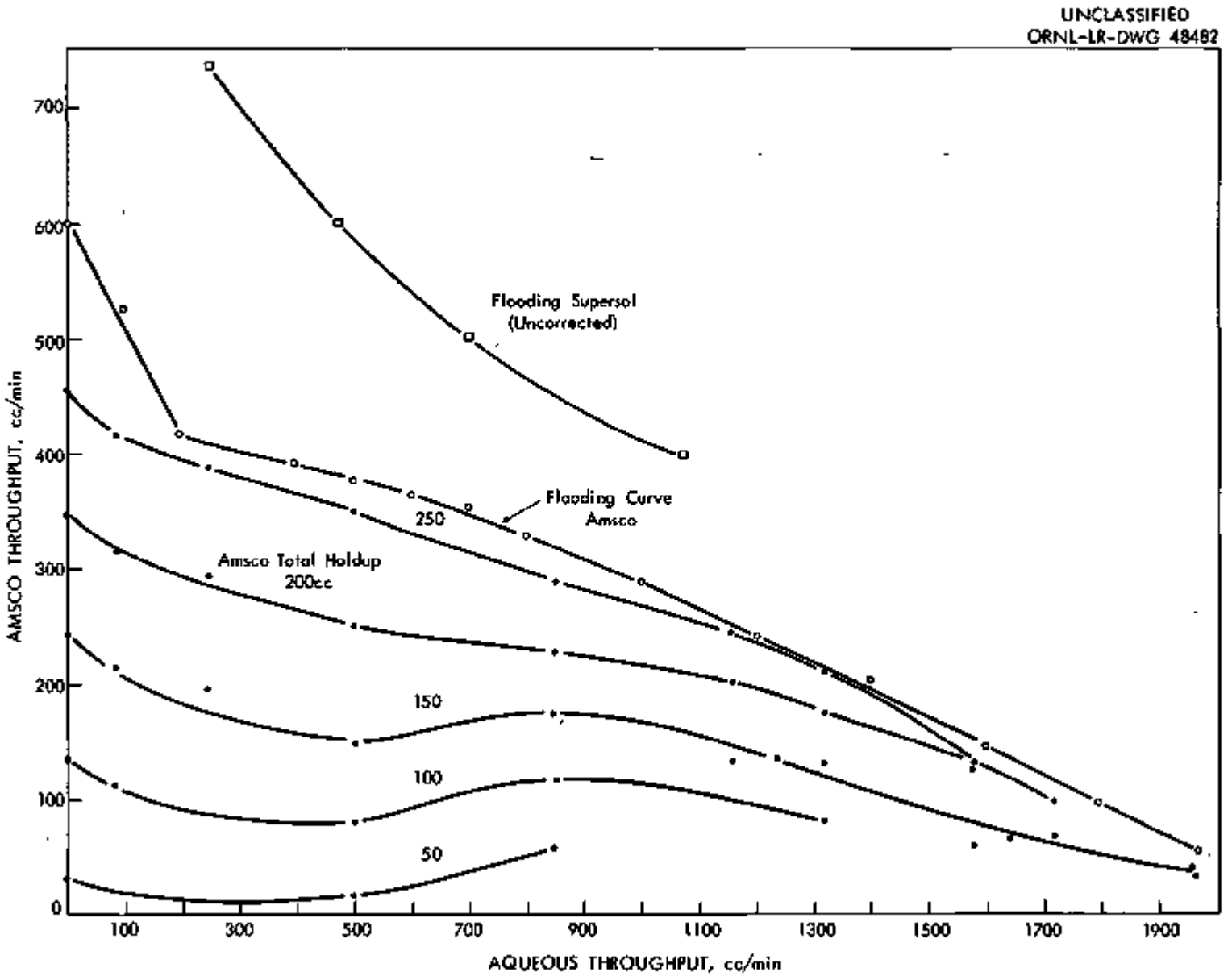

Fig. 2.1. Flooding and holdup curves for Mk I stacked clone contactor with Amsco - 0.08 $M HNO_3$.

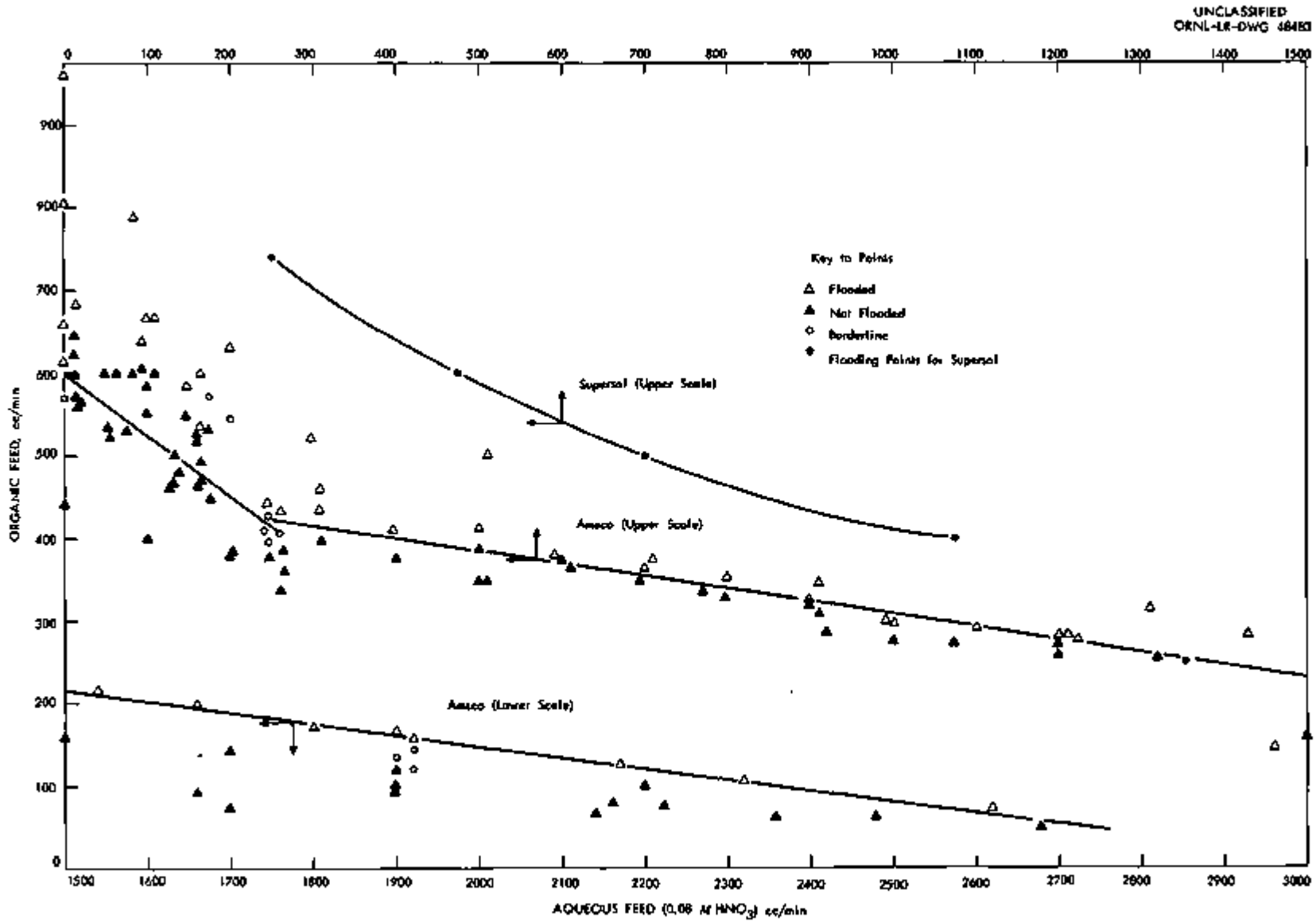

Fig. 2.2. Flooding inputs stacked clone contactor for Amsco - 0.08 *M* and Supersol - 0.08 *M* HNO_3.

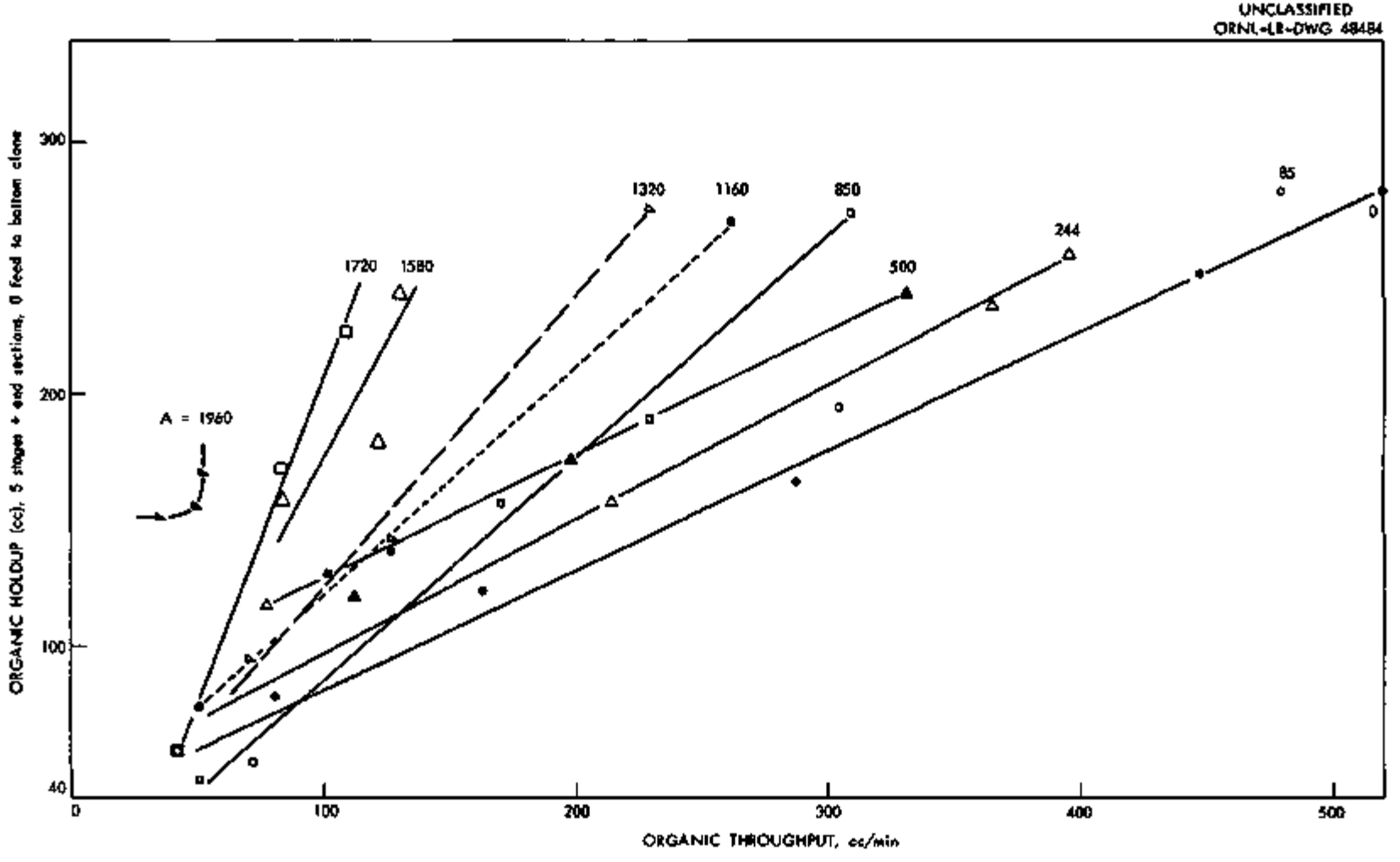

Fig. 2.3. Total organic holdup for MK I stacked clone contactor, five stages + de-entrainer with Amsco – 0.06 M HNO_3.

Table 2.1 and Figure 2.4 present these data. It will be noted that volume per cent of organic in the samples of aqueous is less than 1% except at the highest aqueous throughput. However, at very low O/A a small per cent of entrainment on the basis of the aqueous flow represents a considerable portion of the organic fed. This effect becomes apparent toward the bottom of the last column of Table 2.1 which shows the entrainment as a per cent of organic fed. It should be noted, however, that no attempt was made in any of these tests to return the entrained organic to the contactor and make it go up cascade. The aqueous outlet arrangement is essentially a pipe of clone underflow diameter. Even at the very highest entrainments shown in Table 2.1 the flow rates there shown are steady state conditions with finite throughputs which could be run indefinitely. Arrangements will be tried to keep the now entrained organic in the column by employing one or two clone clarifiers below the organic feed point.

The entrainment of aqueous with organic was very small under all conditions tested.

Table 2.1. Total Amsco Holdup and Amsco Entrainment with the Aqueous (0.08 M HNO_3)

Five Stages and De-Entrainer—Organic Fed to Bottom Clone

Aqueous Input, cc/min	Organic Input, cc/min	Total Holdup, cc	Entrainment		
			cc Amsco per 250 cc Aqueous Outlet Stream	Amsco Vol % of Aqueous Outlet Stream	Amsco Entrained Vol % of Organic Fed
82	305	194	0.30	0.12	0.03
84	480	280	0.10	0.04	0.07
244	78	116	1.00	0.40	1.25
244	214	157	0.60	0.24	0.18
243	365	235	0.58	0.23	0.16
244	397	256	0.90	0.36	0.22
500	115	120	0.61	0.25	1.07
500	200	174	1.00	0.40	1.00
500	335	240	1.56	0.63	0.93
840	54	48	1.00	0.40	6.21
850	78	55	1.28	0.51	5.60
830	176	157	1.36	0.54	2.56
840	230	191	1.35	0.54	1.97
840	315	272	1.27	0.51	1.36
1160	57	76	1.30	0.52	10.60
1160	109	129	1.45	0.58	6.18
1170	133	139	1.32	0.53	4.66
1160	272	269	1.80	0.72	3.10
1320	80	96	1.50	0.72	9.90
1320	136	143	1.55	0.74	6.00
1300	240	274	1.95	0.93	4.22
1580	100	157	2.40	1.43	15.80
1580	133	160	1.90	0.95	16.00
1720	53	59	1.60	0.76	20.70
1760	138	170	7.75	3.07	39.95
1720	207	225	14.20	6.75	47.10
1950	69	155	2.50	1.00	28.50
1950	115	150	6.97	2.80	47.20
1950	147	168	11.95	4.78	64.05
1960	52	152	2.15	0.86	32.50
1960	65	-	2.10	0.84	25.40
1960	160	170	4.40	1.76	21.50

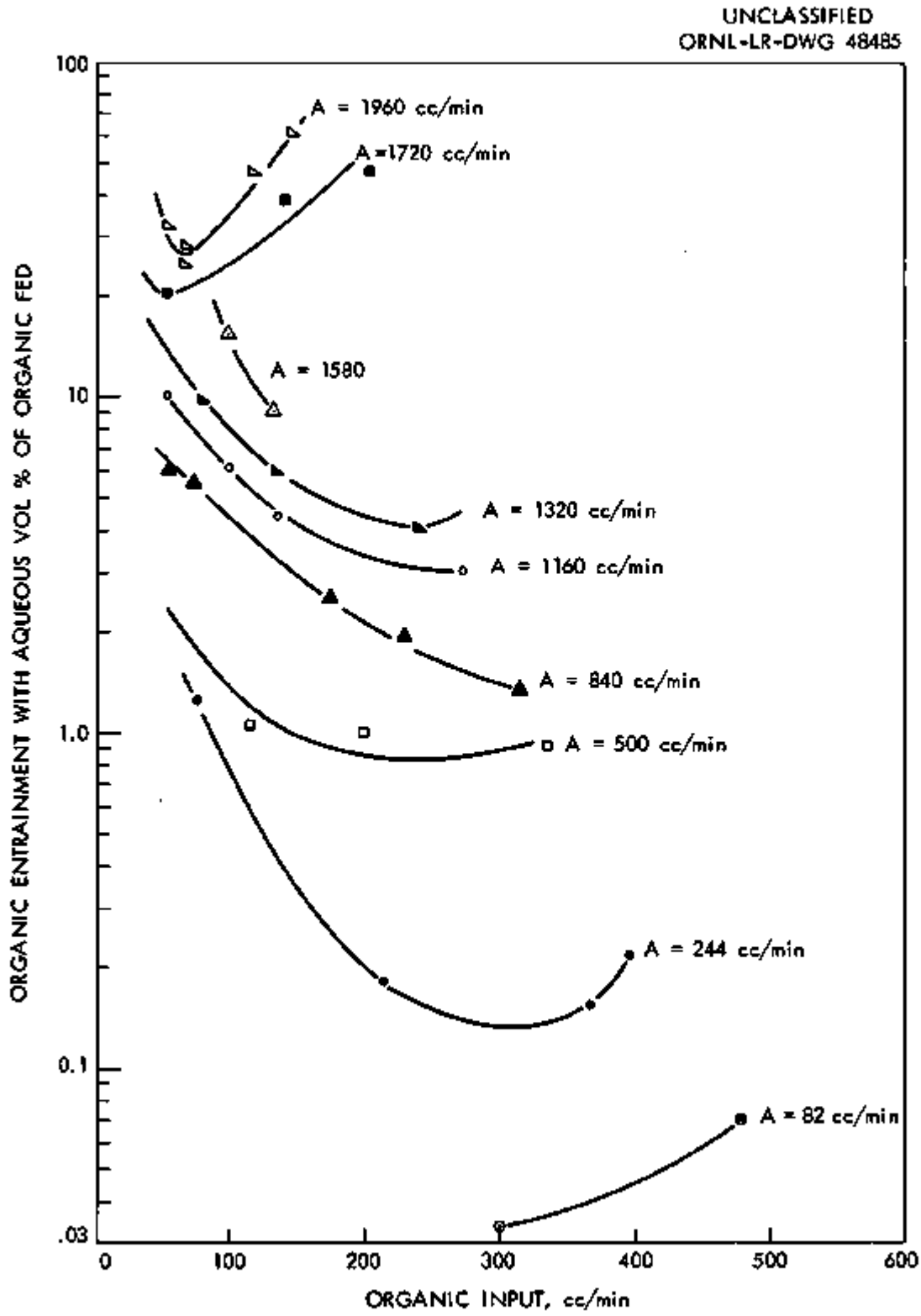

Fig. 2.4. Organic entrainment with aqueous as percent of organic fed. Stacked clone contactor 5 stages and de-entrainer organic fed to bottom clone.

3.0 FUEL CYCLE DEVELOPMENT

P. A. Haas

In order to develop recycle procedures for the fuel and fertile materials used in power reactors, studies are being conducted on fuel element fabrication procedures economically adaptable to remote operation. The initial emphasis is on vibratory compaction of ThO_2 or ThO_2-UO_2 for application with the U^{233}-thorium cycle. Mixed, sized fractions of high density ThO_2 or ThO_2-UO_2 powders are loaded in single stainless steel tubes and vibrated using standard commercial equipment in order to correlate the conditions and results.

3.1 Pneumatic Vibrator Compaction Studies - S. D. Clinton, W. S. Ernst, Jr., J. W. Snider, R. D. Arthur

Eleven runs were made with a "BH - 1-1/4 inch impact type" NAVCO vibrator in an effort to increase the compacted density of fused thoria-urania powders in stainless steel tubes (Table 3.1). The vibrated bulk density of the oxide powders in 3/8-in. dia tubes (2 ft long) varied between 8.5 and 8.9 g/cc. The variation in the vibrated densities can partially be attributed to such factors as the degree of premixing of the different particle size fractions and the uncertainty of loading the tubes uniformly. However, it appears from the results in Table 3.1 and in the Unit Operations March monthly report, a high impact, low frequency vibrating mode is apparently an effective means for compacting powders in long tubes.

The particle size distribution of the fused oxide has been a variable of major interest, however, from the results of Table 3.1 the use of narrow size fractions may not be as necessary as was previously thought. Run 24A is an example of a size distribution including material less than 74 and up to 3360 microns; and, although the size distribution shows four peaks over this range, this run may indicate that high vibrated densities can be obtained with broader particle size ranges. The fine fraction in run 29A was ball-milled for 24 hours which should have given a smaller mean particle size. This particular run vibrated to a density of 8.84 g/cc as compared to a vibrated density of 8.56 g/cc in run 30A in which the fine fraction was not ball-milled.

Run 20E was made to study the effect of particle shape on the vibrated density. The fused oxide particles for the coarse fraction (-10 +16 screen size) were "hand-picked" in order to eliminate any irregular shaped particles which might cause unnecessary bridging. The vibrated density of this run, however, did not show a significant increase.

The tubes were filled by pouring the fused powders through a funnel with the vibrator running. Run 21A was made with no premixing of the coarse, medium, and fine size fractions, and apparently sufficient mixing took place in the 3/8-in. tube to give a reasonably high bulk density (8.52 g/cc). Run 25B was unique in that the fused oxide powder for loading was made into five identical batches of 40 g each. Each batch was mixed and loaded separately into the same tube such that the net result was 200 g of oxide vibrated to a bulk density of 8.86 g/cc. A vibrated density for each loading gave a

Table 3.1. Bulk Densities of Oxide Powders Compacted in Tubes by Means of Pneumatic Vibration Equipment

Conditions: The oxide powders were vibrated in 3/8-in. stainless steel tubes (2 ft long and 35 mil wall thicknesses). The tubes were clamped at the base by means of a Swagelok to pipe connector. All of the runs were made with a BH - 1-1/4 inch NAVCO vibrator at a frequency of 77 cycles per sec. Runs 18-A and 19-A were made with fused ThO_2 while the rest of the runs were made with fused ThO_2-3.4 wt % UO_2.

Run No.	Wt % of U.S. Sieve Fractions						Vibration Time	Vibrated Density	Comments
	Coarse		Medium		Fine				
	wt %	Fraction	wt %	Fraction	wt %	Fraction	min	g/cc	
18A	60.1	10/16	15.2	70/100	25.0	-270	10	8.52	
19A	58.0	10/16	15.2	70/100	26.8	-200	10	8.40	
20E	58.0	10/16	15.2	70/100	26.8	-200	10	8.55	The coarse particles were hand picked.
21A	58.0	10/16	15.2	70/100	26.8	-200	10	8.52	Added coarse, medium, and fine fractions with no premixing
24A	24.5	6/12	27.2	8/16	30.4	-200[a]	10	8.86	1 ft length was seal welded and given to D. E. Ferguson
25A	65.0	10/16	20.0	70/100	15.0	-200	10	8.53	Static load applied to powder during this run and all succeeding runs.[b]
25B	58.0	10/16	15.2	70/100	26.8	-200	8	9.05	Five 40 g lots of feed were made up and added individually to the same tube. A static load was applied after each powder addition.[b]
	58.0		15.2		26.8		8	8.80	
	58.0		15.2		26.8		8	8.81	
	58.0		15.2		26.8		8	8.81	
	58.0		15.2		26.8		10	8.86	
26A	59.5	10/16	15.9	35/70	24.8	-200	3	7.60	Added 90 g out of a 200 g powder batch to the tube.[b]
							10	8.90	Added the remaining powder.[b]
28A	61.2	10/16	7.3	16/70	31.4	-200	13	8.93	b
29A	58.0	10/16	15.2	70/100	26.8	-200	10	8.69	-200 fraction was ball-milled for 24 hrs.
							13	8.84	b
30A	58.0	10/16	15.2	70/100	26.8	-200	10	8.33	
							13	8.56	b

a. Remainder was 17.9 wt % of 40/70 fraction.
b. Static loads were applied by insertion of a 1/4-in. dia rod tapped by weights.

variation of ± 1 to 2 per cent at the various powder depths in the tube. Run 26A was made by adding 90 g of a premixed 200 g loading to a vibrating tube, measuring the bulk density, and then adding the remainder of the fused oxide to the tube. The vibrated density after adding 90 g to the tube was only 7.60 g/cc, however, the bulk density increased to 8.90 g/cc after pouring the entire 200 g batch into the tube. The variation in the two measured densities indicates a high degree of segregation while pouring the powder.

A static load was applied to the surface of the fused powder by means of a 1/4-in. rod tapped by a weight during run 25A and all the succeeding runs shown in Table 3.1. Runs 29A and 30A best illustrate the effect of the static loading. For these two runs a static load was applied to the powder only during the last three minutes of vibration. The bulk densities with no load applied were 8.69 and 8.33 g/cc, while the final vibrated densities of runs 29A and 30A were respectively 8.84 and 8.56 g/cc. Although any applied load should be transmitted only a few inches into the powder depth, the increase in density of approximately 2 per cent in runs 29A and 30A appears directly attributable to the static loading on the powder.

3.2 Electronic Vibration Compaction Studies

The Army permitted the use of an electronic vibrator at Redstone Arsenal, Huntsville, Alabama, on March 31 and April 1. This gave an opportunity to compare an electronic shaker with pneumatic devices now being used at ORNL. The electronic shaker system used was composed of the following units:

Shaker - MB Model C25HB rated at 5000 pound thrust with a 75 pound armature.

Amplifier - Ling Model PP 40/40 rated at 40 kw.

For this study the mixed fused ThO_2-3.4 wt % UO_2 grain was used. The particle size distribution of the grain used was the same as that employed in prior experiments at ORNL which was 58 wt %, 10/16; 15.2 wt %, 70/100; and 26.8 wt %, -200 mesh. Twelve separate batches were made up each consisting of the above particle size distribution. The batches weighing 200 g each were loaded into 2 ft long tubes and two weighing 500 g each were loaded into 5 ft long tubes. The loading was by slowly pouring the material into a tube while it was being vibrated. This loading operation took one minute for the 2 ft tubes and two minutes for the 5 ft tubes. The density of the material after loading is shown in Table 3.2. Rods were inserted into the tubes until the rod rested on the material and were locked in place with a Swagelok fitting. This technique was employed so that spillage would be minimized and the initial density maintained during the trip to Huntsville by auto.

Various vibrating conditions used at Redstone and the densities obtained are given in Table 3.2. It was found that the maximum density, 8.5 g/cc, was obtained for both a 2 ft tube and 5 ft tube when a distorted sine wave input was used. Figure 3.1 shows the acceleration versus time for the armature on which the tube was mounted. The 8.5 g/cc compares with 8.9 g/cc obtained in similar tubes by using pneumatic devices.

Table 3.2. Electronic Vibrator Conditions and Results

Run No.	Tube Length ft	Acceleration gees	Displacement mils	Frequency cycles/sec	Wave Form	Loaded[a] Density g/cc	Electronically[b] Vibrated Density g/cc	Pneumatically[c] Vibrated Density
2	2	60	0.2	2000	Sine	8.33	8.29	8.62
3	2	46	1.0	943[d]	Sine	8.32	8.26	-
4	2	50	160	77	Sine	8.37	7.94	8.26
5	2	50	6	370	Saw-tooth	8.34	8.37	8.50
6	2	48	10	290	Saw-tooth	8.40	8.44	8.69
7	2	19	150	40	Saw-tooth	8.38	8.40	8.75
8	2	29	-	(50-1000)[e]	Random noise	-	8.37	-
9	2	10	-	(50-1000)	Random noise	8.30	8.34	8.62
10	2	20	-	90	Distorted sine	8.44	8.51	8.58
11	2	20	-	66	Distorted sine	8.34	8.23	8.70
12	5	20	-	195	Distorted sine	8.21	8.52	8.62
13	5	10	-	195	Distorted sine	8.23	8.43	8.60

a. One minute vibration for 2 ft tubes and 2 minute vibration for 5 ft tubes while grain was poured into the tubes.

b. Vibrated for 10 minutes.

c. Ten minute vibration after returning to ORNL with BH - 1-1/4-in. vibrator.

d. The natural frequency of a 3 ft section of tube; this was believed close to the natural frequency for a 2 ft tube.

e. All frequencies outside of this range were removed by filters.

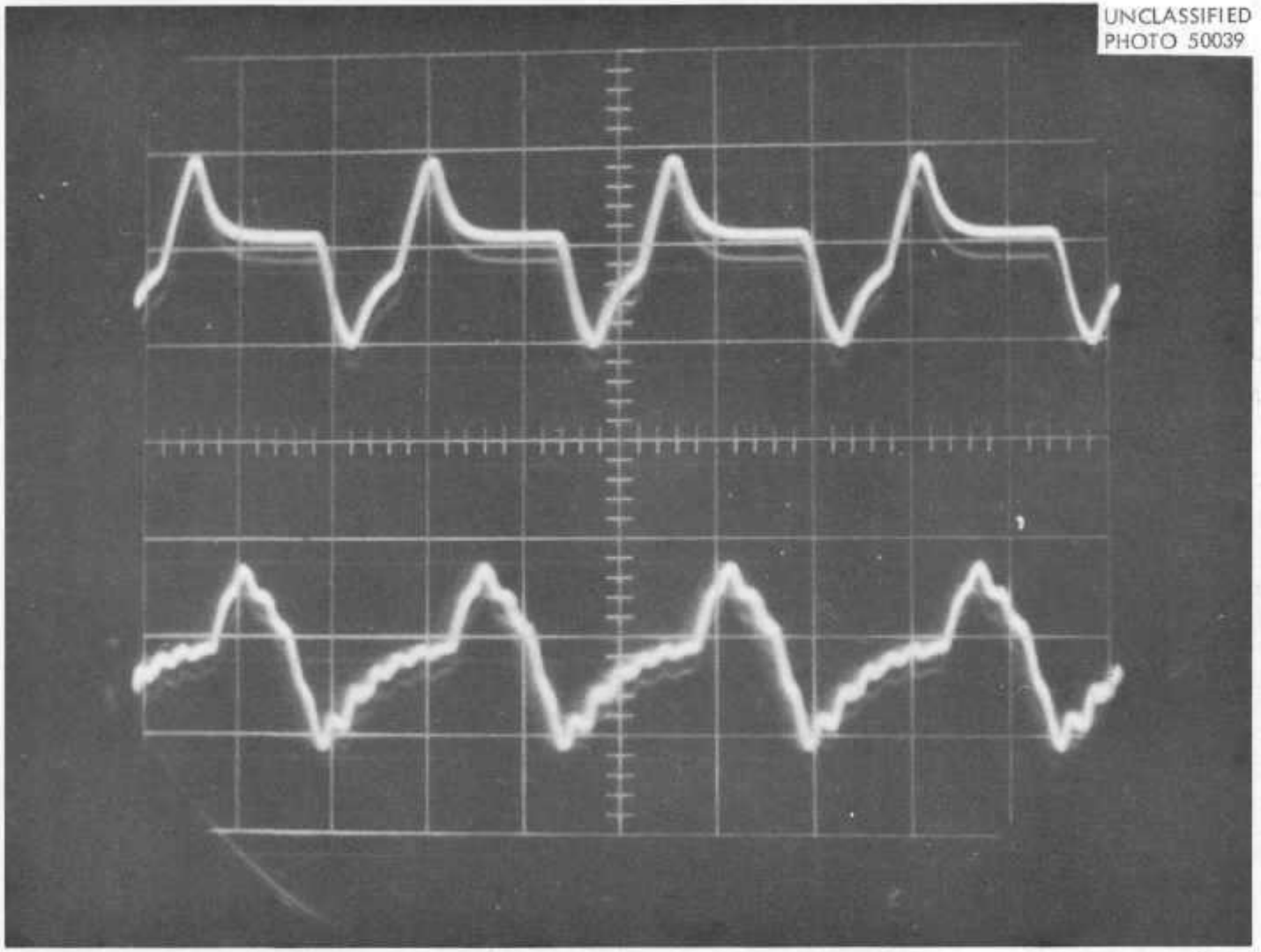

Fig. 3.1. Oscilloscope trace of acceleration vs time of a distorted sine wave input signal. Top trace is from velocity pickup mounted internally to armature. Bottom trace is from accelerometer mounted at the base of the tube. Bottom image is inverted from true signal which results in a short rise time and a slow two-step decay. Basic frequency is 195 cps.

A pure sine wave input had a tendency to decrease the loaded density (Table 3.2) and the saw-tooth, Figure 3.2, and random noise wave forms had little or no effect on density. There were no gross affects attributable to differences in acceleration or frequency, except at low frequencies where the displacement was large.

The same tubes were returned to ORNL and vibrated for 10 minutes with the BH - 1-1/4-in. NAVCO vibrator. Density increases of from 0.1 to 0.5 g/cc occurred over that achieved with the electronic vibrator. The average density of nine tubes, excluding run 4 which appears to be an unusual one, after electronic vibration was 8.39 g/cc and the same tubes after pneumatic vibration had a density of 8.63 g/cc or an average increase of 0.24 g/cc.

A 2 ft tube, run 7, and a 5 ft tube, run 12, were cut open for measurements of densities and particle degredation (Table 3.3). The density difference between the top half and bottom half was 0.2 g/cc for the 2 ft tube and 0.09 g/cc for the 5 ft tube.

The density gradient for the two tubes was reversed with the bottom half of the 2 ft tube denser than the top half, and the top half of the 5 ft tube denser than the bottom half.

Screen analysis reveals that the 70/100 fraction was degradated to produce 1.5 wt % 100/200 in both tubes and the 10/16 fraction degraded to produce about 1 and 2 wt % 16/70. It is interesting to note that this degradation did not result in a significant increase in the amounts of -200 material.

If the initial loading resulted in a uniform distribution throughout, the screen analysis indicates that particle migration occurred. The 10/16 fraction migrated downward in the tube and the -200 fraction migrated upward. The fact that all of the initial loadings were distributed over a 1.4 per cent spread in density indicates a uniform initial distribution.

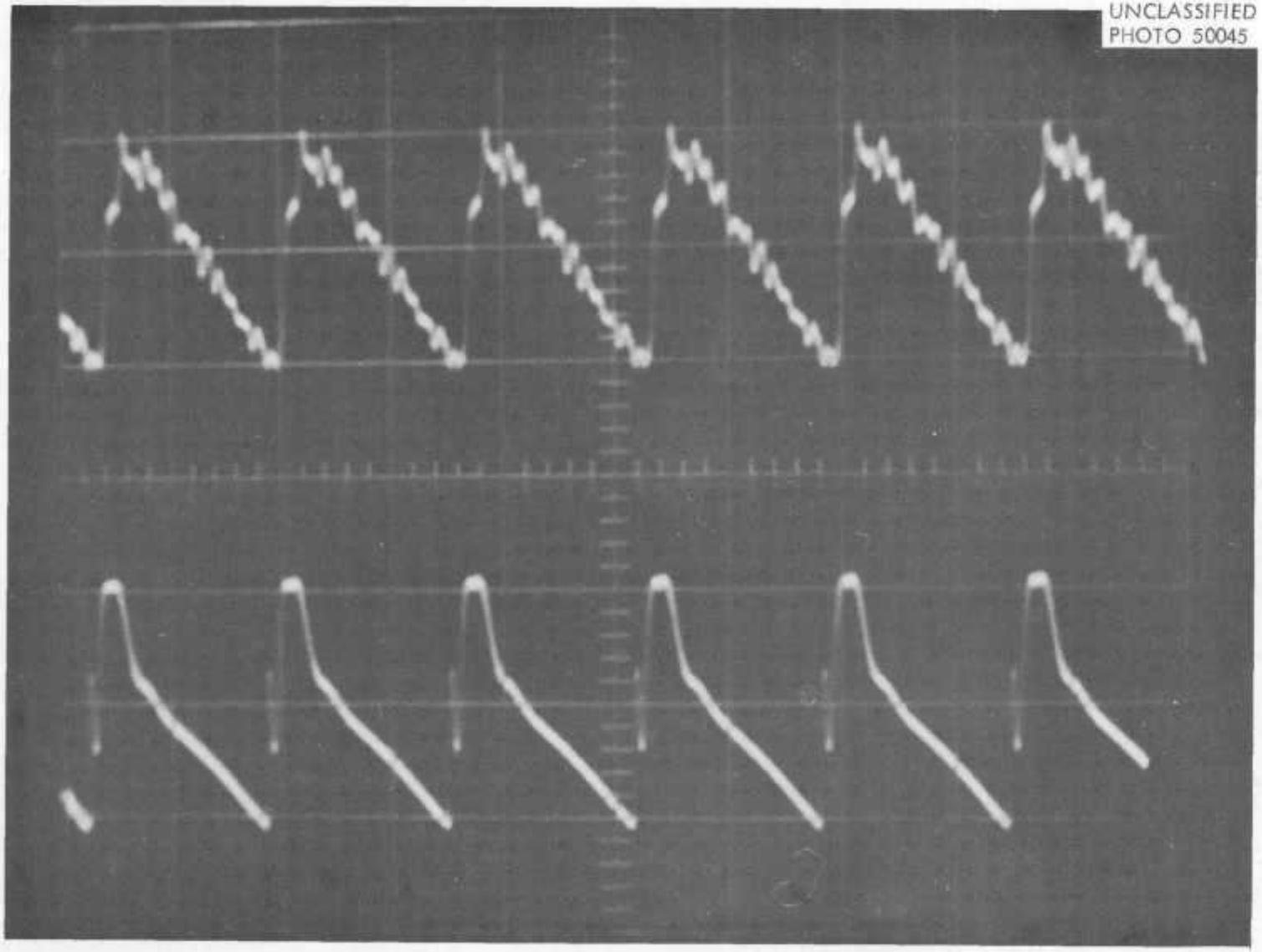

Fig. 3.2. Oscilloscope trace of acceleration vs time of a saw tooth wave form. Top trace is from accelerometer mounted at the base of the tube. Bottom trace is from velocity pickup mounted internally to the armature. Basic frequency is 370 cps with a fast rise time and slow decay.

Table 3.3. Particle Size Analysis and Density Measurements for Segmented Tubes

Vibration time: One minute while loading 2 ft tube, 2 minutes while loading 5 ft tube, 10 minutes electronically and 10 minutes pneumatically for 21 or 22 minutes total.

Material: Fused ThO_2 - 3.4 wt % UO_2

a. Screen Size Analyses for Whole Tubes

Screen Size U.S. Standard	Initial	Run No. 7[a]	Run No. 12[b]
10/16	58.0 wt %	55.7 wt %	57.0 wt %
16/70	-	1.7 wt %	0.9 wt %
70/100	15.2 wt %	13.9 wt %	13.7 wt %
100/200	-	1.4 wt %	1.5 wt %
-200	26.8 wt %	27.4 wt %	26.9 wt %

b. Screen Size Analyses for Tube Segments

Screen Size U.S. Standard	Run No. 7[a]		Run No. 12[b]	
	Top	Bottom	Top	Bottom
10/16	52.3 wt %	58.6 wt %	52.3 wt %	61.9 wt %
16/70	2.0 wt %	1.4 wt %	0.6 wt %	1.1 wt %
70/100	14.3 wt %	13.4 wt %	15.4 wt %	12.0 wt %
100/200	1.5 wt %	1.3 wt %	1.4 wt %	1.5 wt %
-200	29.6 wt %	25.3 wt %	30.3 wt %	23.6 wt %
Density	8.62 g/cc	8.82 g/cc	8.68 g/cc	8.59 g/cc
Density prior to Segmenting	8.76 g/cc		8.63 g/cc	

a. 2 ft tube length.

b. 5 ft tube length.

4.0 GCR COOLANT CLEAN-UP STUDIES

J. C. Suddath

Contamination of coolant gases by chemical impurities and release of fission products from fuel elements is a major problem in gas cooled reactors and inpile experimental loops. Investigations are being made to determine the best methods to reduce the impurities, both radioactive and non-radioactive, with emphasis on chemical impurities in the EGCR coolant and radioactive impurities in EGCR experimental loops.

4.1 EGCR Experimental Loops

Design assistance is being furnished the RPD in the selection of a filter system for particulate removal and a charcoal bed for rare gas holdup for the experimental loops to be installed in the EGCR.

4.2 Helium Purification Test Facility - C. D. Scott

The helium purification test facility which is designed to simulate a purification system for helium contaminated with H_2, CO, CH_4, CO_2, and H_2O has been completed. The initial experimental program in this facility will be an evaluation of a fixed-bed CuO oxidizer for oxidation of small amounts of H_2, CO, and CH_4 in helium.

The CuO oxidizer will be evaluated by determining efficiency of oxidation of the oxidizable contaminates in a flowing stream of helium. All tests will be made on a fixed-bed of CuO and parameters will be investigated to allow establishment of a flow reactor design equation. Analytical grade, 0.017-in.-dia CuO wire will be used in the oxidizers.

The test facility contains two CuO oxidizers in parallel. These oxidizers are fabricated from 2-in. sch. 80 SS pipe with high pressure (600 psi) flanges at either end (Figure 4.1). Any bed depth from 1/4-in. to 12-in. can be maintained and there are thermocouple probes every 2 in. within the vessel. The oxidizer is internally insulated at top and bottom and it is externally heated and insulated by a tube furnace. The operating ranges for the oxidizer are 30-340 psia, 370-570°C and helium flow rates of 1.0 to 100 slpm.

Experimental Results. A total of six experimental runs have been made on the 2-in. dia oxidizer for oxidation of H_2 in helium and results from four of these runs are usable. These runs were made at 45 psia and 300 psia and at bed temperatures of 430 to 446°C. H_2 contamination of 1.0 to 1.3% (by vol.) was used with total gas flow rates of 4.5 to 5.4 slpm (Table 4.1). The main reason for these tests were to check out equipment and operating procedures; however, the last four runs (OH-3 - OH-6) resulted in some usable data. Three of these runs were made at 45 psia and temperatures of 430-446°C with CuO bed depths of 1/4 to 1/2-in. and total gas flow rates of 4.5 to 4.8 slpm of helium with 1.02 to 1.30% hydrogen. An increase in bed depth decreased the minimum H_2 concentration in the off-gas. The one run made at 300 psia and 438°C in a 1/4-in. bed at a flow rate of 5.37 slpm of 1.13% H_2 in helium resulted in a minimum hydrogen concentration in the off-gas of 240 ppm (by vol.).

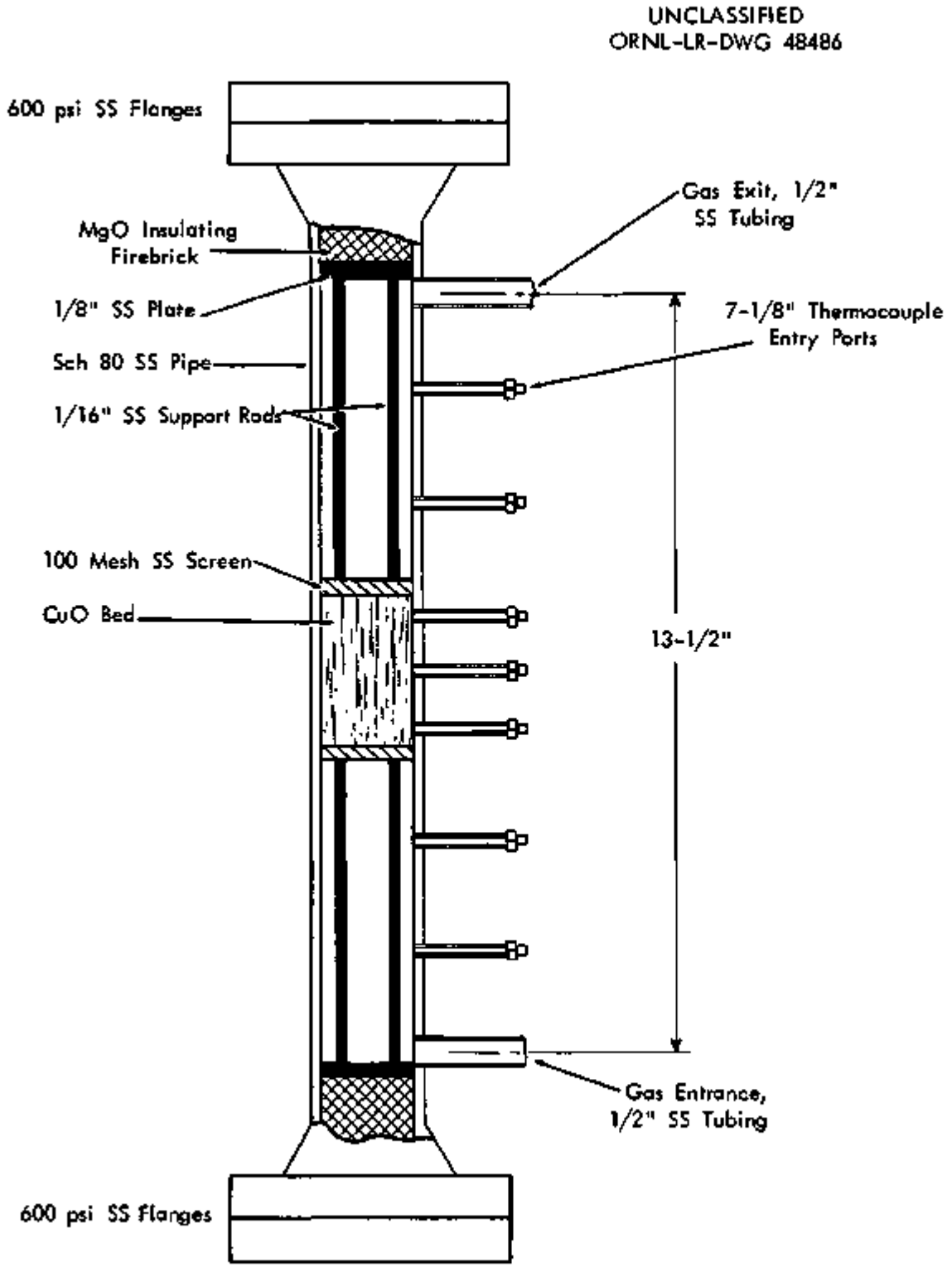

Fig. 4.1. 2-in. oxidizer in helium purification test facility without external heater.

Table 4.1. Experimental Results from Four Runs for Evalution of the CuO Oxidizer for Helium Contaminated with H_2

Run No.	Average Bed Temperature °C	System Pressure, psia	Hydrogen Concentration in Feed Gas, vol %	Gaseous Feed Rate, slpm	Volume of CuO Bed, cc	Maximum Conversion of H_2, % of initial	Run Time at Maximum Conversion of H_2, min
OH-3	432	45	1.30	4.72	24.1	98.5	31
OH-4	446	45	1.13	4.46	24.1	99.5	19
OH-5	443	45	1.02	4.74	12.1	96.0	15
OH-6	438	300	1.13	5.37	12.1	97.9	15

In each run there was an initial period of decreasing hydrogen concentration in the off-gas followed by a period of more gradual increase in hydrogen concentration (Figure 4.2). This first period, a so-called "induction" period, has been noted by other workers[1-4] and it has been postulated that during this period, the active centers of the reaction are growing rapidly. The second period of gradual increasing hydrogen in the off-gas shows the effect of bed depletion.

References

1. W. D. Bond, W. E. Clark, "Reduction of Curpic Oxide by Hydrogen. I. Fundamental Kinetics," ORNL-2815, March 16, 1960.

2. W. D. Bond, W. E. Clark, "Reduction of Cupric Oxide by Hydrogen. II. Conversion of Hydrogen to Water Over Fixed Beds," ORNL-2816, January 29, 1960.

3. A. T. Larson and F. E. Smith, "The Synthesis of Water Over Nickel and Copper Catalysts," J. Am. Chem. Soc., 47: 346 (1925).

4. J. S. Lewis, "The Reduction of Copper Oxide by Hydrogen," J. Chem. Soc., 1932, p. 820.

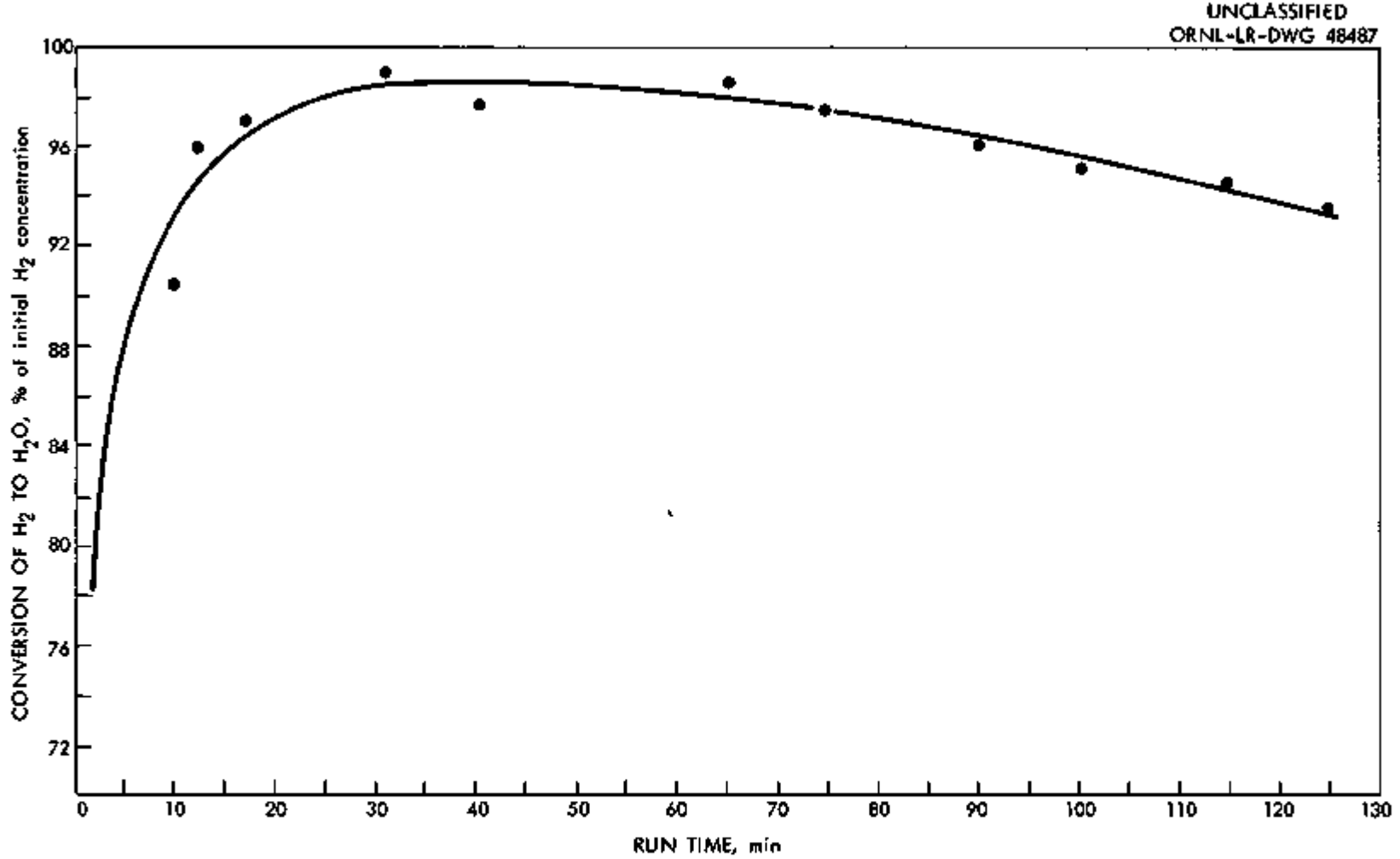

Fig. 4.2. Conversion of H_2 to H_2O in a flowing stream of He by a fixed bed of CuO at 45 psia, 432°C, and 4.72 slpm of He containing 1.3% H_2 through 24.1 cc of CuO bed (Run OH-3).

5.0 HR THORIUM BLANKET STUDIES

P. A. Haas

Studies were continued on the preparation of spherical thoria particles for aqueous slurry blankets and on thoria pellets for pebble bed type blankets. The emphasis for slurry preparation by use of flame denitration is on preparation of 5 to 10μ spherical particles with other properties comparable to those obtained for 1 to 2μ diameter material.

5.1 Flame Denitration - C. C. Haws, Jr., K. O. Johnsson, V. L. Fowler

Significant improvement in the properties of the flame prepared thoria product could be realized by increasing the average particle size from the present 1-2μ dia to the 5-8 micron range. An accompanying benefit of increased process yield might also be obtained from such a particle size increase.

No variable, within the range investigated to date, has shown promise of yielding the desired increase in particle size. Evidence mounts that the liquid feed droplet and/or the large solid particle, explodes and yields hundreds of smaller droplets (or particles) during the decomposition-drying-calcination operation (Table 5.1). This effect is believed to occur as a result of the extremely rapid temperature rise of the feed droplet and the rapid transfer of both heat and vapor through the dried, or drying, particle.

Within the liquid droplet size range (50-150 micron) and the reflector temperature range (900-1500°C) investigated, there is no worthwhile variation in particle size. The use of nitrogen to drive the atomizer, thus avoiding intimate contact of the combustion gases with the atomized feed, had no effect on particle size. The use of water instead of CH_3OH as a solvent for the feed similarly had no effect.

Table 5.1. Particle Size of Flame Calcined ThO_2

Feed: 300 g/liter of $Th(NO_3)_4 \cdot 4H_2O$ in solvent listed.

		Feed Used		Atomizing Gas			Liquid Drop Dia		Mean Particle Dia.		
Run	Reflector Temperature	Solvent	Flow	Material	Flow	Nozzle Velocity	Calculated	Observed	From Calc. Liquid dia	From Obs. Liquid dia	Measured
	°C		cc/min		SCFM	m/sec	μ	μ	μ	μ	μ
96	1500	H_2O	7	N_2	2.19	130	39	50	9	12	1.3
97A	900	H_2O	6	N_2	2.19	130	38	50	9	12	1.6
97B	900	H_2O	30	N_2	2.19	130	47	150	10	36	2.0
98	900	CH_3OH	10	N_2	2.19	130	26	-	6	-	1.7
99A	1500	CH_3OH	30	N_2	2.19	130	37	-	8	-	1.6
99B	1500	H_2O	30	N_2	2.19	130	48	-	10	-	1.2

6.0 ION EXCHANGE

J. C. Suddath

To make rational predictions of the operating characteristics of uranium anion exchange contactors, an understanding of the mechanism and kinetics of the exchange is necessary. Toward this objective the equilibrium sorption isotherms and rates of sorption of uranium on Dowex 21K are being determined.

6.1 Uranium Anion Exchange Kinetics Studies - J. S. Watson

Recent experimental studies have been on the effects of sulfate concentration on the rate of uranyl sulfate loading on nitrate equilibrated resin. Previous work has shown that the rate of loading on sulfate equilibrated resin is essentially independent on the total sulfate concentration in the loading solution. It was not obvious that this should also be the case using nitrate equilibrated resin since these may be conditions under which the sulfate concentration in the resin is not sufficient to convert all of the uranium to anion complexes. Loading runs were made using 1200μ Dowex 21K and two solutions both 0.005 M in uranyl sulfate and 0.020 M in sulfuric acid but with different total sulfate concentrations, 0.050 M and 0.10 M. The different total sulfate concentrations were obtained by adding sodium sulfate. The results of these runs are shown in Figures 6.1 and 6.2. Note that both runs gave apparent uranium diffusion coefficients of approximately 1.6×10^{-7} sq cm/sec. These data combined with a run reported in the February Unit Operations Section monthly progress report for loading from a solution 0.025 M in total sulfate, in which the apparent uranium diffusion coefficient was approximately 1.5×10^{-7} sq cm/sec, indicate that there is little dependence between the loading rate on nitrate equilibrated resin and the loading solution sulfate concentration. This indicates that the sulfate ion which is much more mobile than the uranium complexes, (the sulfate self-diffusion coefficient in 1200μ Dowex 21K is 1.2×10^{-6} sq cm/sec while the uranium self-diffusion coefficient in the resin is approximately 3×10^{-8} sq cm/sec) diffuses into the resin so much faster than the uranium that the uranium appears to be essentially always in sulfate equilibrated resin. The apparent uranium diffusion coefficient is higher when measured during loading on nitrate equilibrated resin than during loading on sulfate equilibrated resin probably because of the greater electrical forces rather than different distribution of the complexes.

Elution runs were made using resin equilibrated with both of the above loading solutions, 1200μ Dowex 21K equilibrated with the 0.005 M uranyl sulfate solution 0.05 M in total sulfate was eluted with a 1 M $NaNO_3$-0.1 M HNO_3 solution. As in most elution runs using the single bead technique, the data was badly scattered, but an apparent uranium diffusion coefficient of approximately 2×10^{-7} sq cm/sec was measured. This is slightly greater than the value of 1.7×10^{-7} sq cm/sec observed using resin equilibrated with a loading solution 0.025 M in total sulfate. However, because of the bad data scatter observed in elution runs, this should not be considered sufficient to show a dependence of elution rate with loading solution concentrations unless more accurate runs using a new contacting device give the same results. Such a dependence appears unlikely.

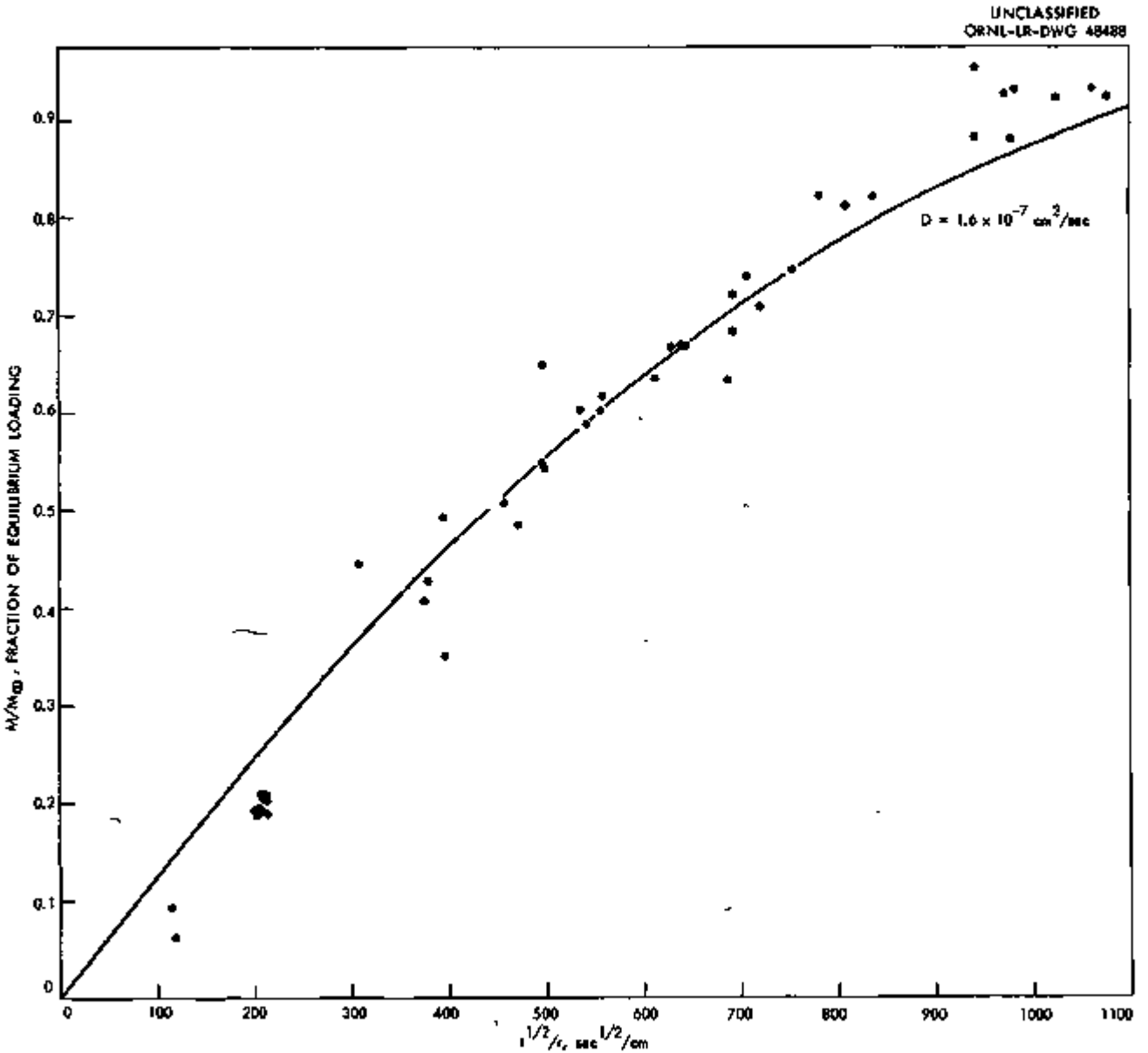

Fig. 6.1. The rate of uranium loading on nitrate equilibrated 1200 μ Dowex-21K from a 0.005 *M* uranyl sulfate solution 0.050 *M* in total sulfate.

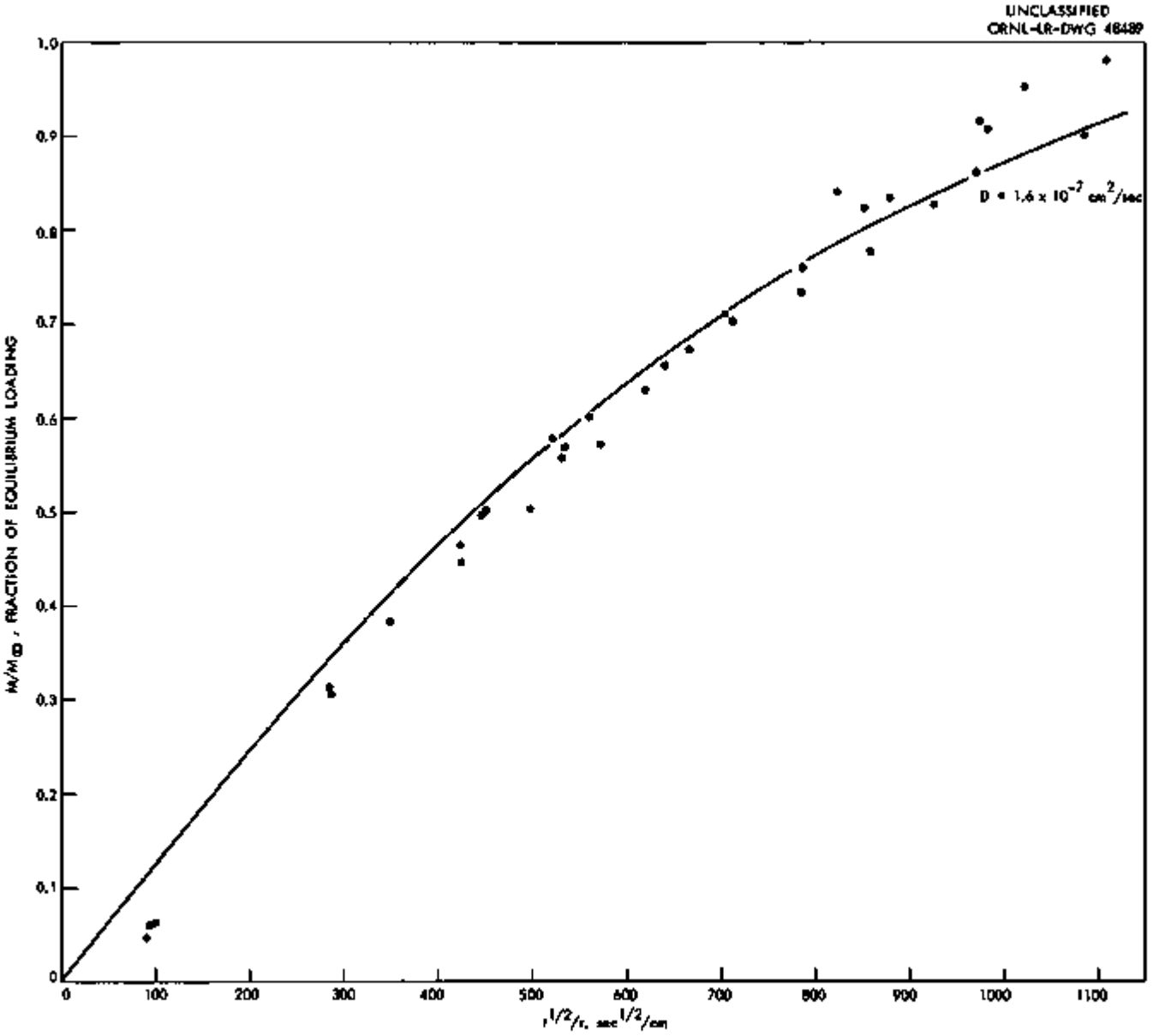

Fig. 6.2. The rate of uranium loading on nitrate equilibrated 1200μ Dowex-21K from a 0.005 *M* uranyl sulfate solution 0.10 *M* in total sulfate.

Resin equilibrated with the 0.005 M uranyl sulfate solution 0.10 M in total sulfate was eluted with a 1 M NaCl-0.1 M HCl solution. The apparent uranium diffusion coefficient was approximately 4×10^{-7} sq cm/sec. There was considerable data scatter, but this result is accurate enough to indicate that elution rates are higher with chloride solutions than with nitrate solutions under the conditions studied.

Other efforts have been directed toward developing a numerical calculation method for describing the ion exchange rates and toward constructing a device to contact small quantities of resin with the loading solution under known flow conditions. This device will allow measurements of the effects of stagnant fibers around the resin on the loading rate, and it will allow enough beads to be contacted with the solution to reduce the effects of nonuniformity of the resin beads. This is particularly important in elution runs and uranium self-diffusion measurements.

7.0 POWER REACTOR FUEL PROCESSING

C. D. Watson

7.1 Darex-Thorex - F. G. Kitts

Darex is an aqueous head end treatment for the conversion of stainless steel alloyed or jacketed fuels into chloride-free nitrate solutions suitable for processing in existing equipment. Chloride is necessary to dissolve stainless steel but it must be removed to avoid corrosion of subsequent processing equipment. Presently, Darex is being evaluated for the processing of stainless steel clad UO_2-ThO_2 ceramic pellets such as Consolidated Edison. Decladding might be accomplished using 5 M HNO_3 - 2 M HCl followed by core dissolution in a standard Thorex solution (13 M HNO_3, 0.04 M fluoride, 0.1 M Al^{+++}), or the Darex decladding solution with chloride removed, HNO_3 adjusted and fluoride added might be used to dissolve the UO_2-ThO_2.

The effect of HNO_3 concentration on the dissolution rate of UO_2-ThO_2 in both Thorex and stainless steel-containing dissolvents was determined.

Four UO_2-ThO_2 dissolution runs were made in a 1-in. dissolver using a technique wherein a batch of dissolvent is continuously recirculated between a refluxing flooded dissolver and a well-mixed external reservoir. Two types of dissolvents were evaluated at two nitric acid concentrations. Data for the four runs are shown in Table 7.1 and Figure 7.1. Runs SS-3 and 4 were made with a dissolvent containing 53 g SS/liter, 0.04 M fluoride and 13.2 and 15.1 M HNO_3; runs Th-12 and 13 were made using Thorex solutions containing 0.04 M fluoride, 0.1 M Al^{+++} and 13.2 and 15.5 M HNO_3. A standard 8 hr dissolution time was used with the dissolvent recirculated at the rate of 3-1/2 - 4 cc/min; only ~50% dissolution was accomplished in all runs resulting in lower than anticipated product loadings. A decrease in the dissolvent volume was noted in all cases with larger discrepancies observed for the stainless steel dissolvent and for the higher HNO_3 concentrations. These probably signify greater losses due to decomposition, especially since 90% HNO_3 was used to prepare the SS dissolvent.

The average dissolution rates (item 9, Table 7.1) were calculated from the expression:

$$R = \frac{3W_o}{A_o T}\left[1 - \left(\frac{W}{W_o}\right)^{1/3}\right]$$

where:

R = dissolution rate (mg/sq cm-min)

W_o = initial weight of pellets (g)

A_o = initial area of pellets (sq cm)

T = refluxing time (min)

W = weight of pellets after time T (g)

Table 7.1. Data for Recycle Dissolution of UO_2-ThO_2 Pellets in the 1-in. Dissolver

8 hour dissolution time

		SS-3	SS-4	Th-12	Th-13
1.	Weight of UO_2-ThO_2* charged (g)	85.80	85.92	86.48	86.49
2.	Weight of UO_2-ThO_2 dissolved (%)	55.80	47.43	41.52	44.54
3.	Weight of UO_2-ThO_2 undissolved (g)	37.92	45.17	50.57	47.96
4.	Initial HNO_3 in dissolvent (M)	13.2	15.1	13.2	15.5
5.	Dissolvent volume (cm^3)	393	393	393	393
6.	Final product volume (cm^3)	359	350	372	365
7.	Final product loading (g Th/liter)	105	99.4	78.6	84.2
8.	Initial Area (16 pellets)(cm^2)	65.15	65.20	65.50	65.57
9.	Average dissolution rate $\left(\frac{mg\ UO_2\text{-}ThO_2}{cm^2\text{-}min}\right)$	1.97	1.60	1.36	1.48

* 16 cylindrical pellets, 4.4% UO_2, Den = 9.51 ± 0.04 g/cm^3, O/U = 2.00, supplied by Universal Match Co.

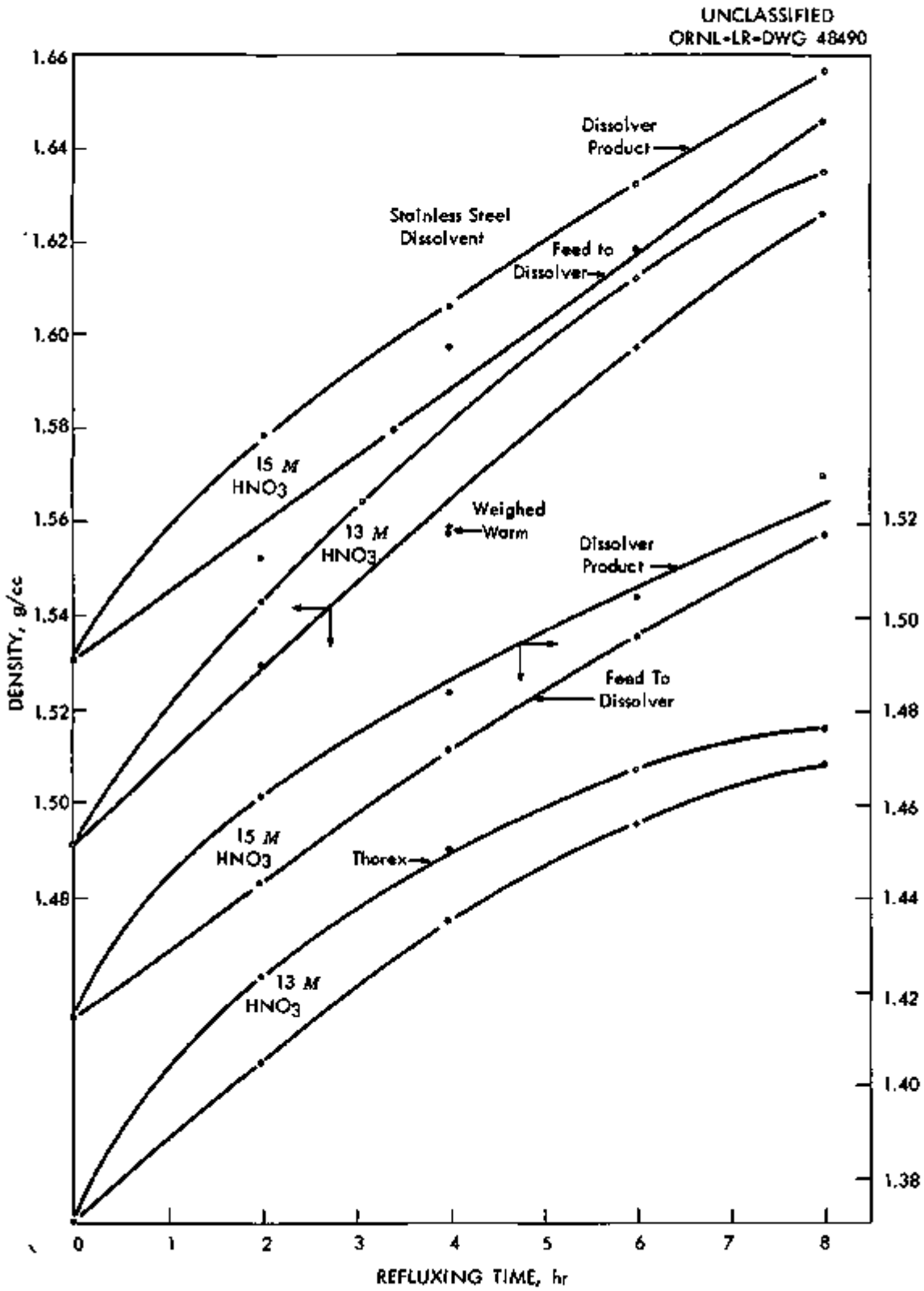

Fig. 7.1. Increase in density of UO_2-ThO_2 dissolvents with processing time.

This is the integrated form of the rate equation R = W/AT assuming that R is constant over the time T and utilizing the proportionality A = $kw^{2/3}$. (This assumes pellet length = pellet diameter which is permissible since only ~50% dissolution was accomplished. Actual L/D ≅ 2.4).

In Figure 7.1 the densities of the dissolver products and reservoir contents are plotted as a function of refluxing time (recirculation was also begun when refluxing began). Since the density is proportional to loading, material balances at any time may be calculated from the volumes involved and the density-loading relationship. This work was of an exploratory nature since neither the Universal Match Company pellets nor stainless steel dissolvents with >10 M HNO_3 had been investigated previously. The upper curve in each pair (Figure 7.1) shows the density of the contents of the flooded dissolver (hold-up 70-75 cc) and the lower line represents the density of the solution in the reservoir (280-320 cc). The vertical distance between a pair of lines denotes the amount of dissolution being accomplished at any time and is a function of the instantaneous dissolution rate and the recirculation rate. Since the recirculation rate is constant throughout any run (and reasonably reproducible between runs) this distance as well as the slope of the line may be considered proportional to the product RA; over short periods the area may be assumed constant so the slope depends only on the reaction rate. In the case of the SS dissolvent the lines are essentially straight indicating a constant RA; from this it might be inferred that higher dissolutions (%) might be accomplished by increasing the reflux time proportionally. However, with the 13 M Thorex dissolvent the RA is observed to be consistently decreasing indicating that higher % dissolutions will be increasingly harder to achieve. The data for the two Thorex solutions indicate that the optimum dissolvent (ratewise) should have >13 M HNO_3.

Since interest at this time is concentrated primarily on the Thorex route, no further immediate work is contemplated with the stainless steel dissolvents. Instead, a study of the instantaneous dissolution rates of UO_2-ThO_2 (UMC pellets) has been initiated in an effort to obtain fundamental data which will permit the reaction rate to be expressed as a function of the Th and HNO_3 acid concentrations in the Thorex dissolvent. Nitric acid concentrations from 8-18 M with Th loadings up to 1.0 M will be investigated with fluoride and Al^{+++} held constant at levels of 0.04 and 0.1 M, respectively. Uranium will be present in the ratio of Th/U = 20.

7.2 Sulfex - B. C. Finney, T. D. Napier

Stainless steel clad UO_2-ThO_2 and UO_2 power reactor fuels may be processed by the Sulfex process. The clad metal is dissolved in boiling 4-6 M H_2SO_4; the core in boiling nitric acid (for UO_2) or fluoride catalyzed nitric acid (for UO_2-ThO_2 mixtures). The application of the Sulfex process to the NMSR and Consolidated Edison fuels is being investigated.

Two additional semi-continuous cyclic Sulfex declad (SX-34 and 36) and Thorex core dissolutions (SX-35 and 37) of prototype Consolidated Edison fuel assemblies were made. These runs were a continuation of the series of runs reported in Unit Operations Section monthly progress report, Marcy 1960 (CF 60-3-61). The run data are summarized in Table 7.2.

Table 7.2. Sulfex Cyclic Decladding and Core Dissolutions

Dissolver Charge: Two prototype Consolidated Edison fuel assemblies[1]

(Declad)

Run No.	Time Hrs	Dissolvent Composition	Vol ℓ	Flow Rate ℓ/min	Stainless Steel 2 assemblies + heel, g	Stainless Steel Dissolved g	Stainless Steel Dissolved %	Solids Collected in Centrifuge g	Heel S.S. + braze g	F/θ cm/min	Average Reaction Rate mg/cm²-min	Product Losses to Declad H+ M	Product Losses to Declad g S.S./ℓ	Product Losses to Declad HNO_3 M	Product Losses to Declad Th %	Product Losses to Declad U %
SX-34	3.3	4 M H_2SO_4	122	0.613	4434	4066	91.7	60	308	0.06	2.0	3.53	33.3	~0.001	0.2	0.02
SX-36	3.9	4 M H_2SO_4 0.1 M HCOOH	156	0.661	4364	4056	92.9	60	248	0.065	1.7	3.60	26	~0.001	0.25	0.04

(Core Dissolution)

Run No.	Time Hrs	Dissolvent Composition (initial)	Vol ℓ	Flow Rate ℓ/min	Core Wt UO_2-ThO_2 + heel, g	Core Dissolved Th g	Core Dissolved Th %	Core Dissolved U g	Core Dissolved U %	Heel[2] UO_2-ThO_2 g	Reaction Rate mg/cm²-min	Product Composition H+ M	Th g/ℓ	U g/ℓ	$SO_4^{=}$ M	Cr M	Ni M	Fe M	F^- M	$PO_4^{\equiv}$ M	B M	Cd M	Al M
SX-35	10	13.4 M HNO_3 0.04 M F^- 0.12 M Al 0.06 M B	66	1.45	12957	8924	85	478	90	2260	1.9	9.71	126	6.76	0.001	0.006	0.01	0.006	0.04	0.002	0.05	-	0.11
SX-37	9.5	12.7 M HNO_3 0.04 M F^- 0.10 M Al 0.025 M Cd 0.06 M B	65	1.43	13874	9075	80	508	80	2971	2.05	9.4	137	7.7	0.007	0.0006	0.01	0.009	0.04	0.005	0.06	0.021	0.10

1. Each fuel assembly consists of 36-25 inch long x 5/16 inch o.d. x 0.020 inch wall thickness 304 stainless steel tubes filled with UO_2-ThO_2 pellets (Davison 95.6% ThO_2-4.2% UO_2) ρ ≈ 9.6 g/cc, N_2 annealed - wt of stainless ≈ 2025 g - outside surface area ≈ 5100 cm^2 - tubes brazed together using 2 rows of ferrules and Microbraz 50 UO_2-ThO_2 ≈ 5800 g.

2. Weight of heel based on known weight charged to dissolver and analysis of core solution - actual weight of heel at conclusion of SX-37 was 2058 g of which approximately 1600 g was UO_2-ThO_2 pellet fragments (5.6% of total weight of pellets charged to dissolver).

The dissolver charge consisted of two prototype Consolidated Edison fuel assemblies plus the heel remaining from the previous run. The clad dissolvent was boiling 4 M H_2SO_4 and the core dissolvent was fluoride catalyzed HNO_3. Average stainless steel reaction rates during decladding varied from 1.7 - 2.0 mg/sq cm-min at a dissolvent flow rate/initial outside surface area (F/S) of approximately 0.06. One of the fuel assemblies in run SX-34 had been autoclaved for 7 days at 300°C and 2000 psig (steam + O_2) to oxidize the surface. This particular fuel assembly behaved no differently than the unoxidized assemblies. Although these fuel assemblies were initially passive to the boiling 4 M H_2SO_4 dissolution began immediately after the dissolver was drained (~10 liters) and fresh dissolvent was introduced. Apparently the passivation was induced by an excessive nitrate ion concentration (0.06 NO_3^- in the discharged dissolvent). Passivation of this same nature had been encountered in run SX-32. The dissolvent in run SX-36 was "spiked" with 0.1 M HCOOH and dissolution started as soon as the boiling dissolvent contacted the fuel assemblies. The washing procedure had not been changed, consequently it is assumed that a passive condition existed prior to declad run SX-36 as it did prior to runs SX-32 and 34. Based on the results of this run it appears that HCOOH warrants consideration as a depassivation reagent to destroy small quantities of NO_3^-.

The thorium loss to the declad solution was approximately 0.2% and the uranium loss varied from 0.02 - 0.04%. There was approximately a 10 fold increase in the thorium loss when decladding in the presence of a UO_2-ThO_2 heel as compared to a no heel (0.02 versus 0.2%) whereas the uranium loss was relatively constant (0.02 - 0.04%) with the exception of run SX-32 in which the loss was 0.1%.

Core dissolution runs SX-35 and 37 were made recycling the dissolvent through the dissolver. It has been proposed to control criticality in the PRFPPP by using either boron and/or cadium as nuclear poisons. The dissolvent was "spiked" with boron in run SX-35 and with both boron and cadium in run SX-37. The data indicate that neither boron nor cadium are lost through volatilization or precipitation during the core dissolution.

Each run was made using approximately 65 liters of dissolvent at an average external recirculation rate of 1.43 liters/min and a run duration of approximately 10 hours. An analysis of the core solution at the conclusion of each run indicated that approximately 85% of the dissolver charge (UO_2-ThO_2 pellets + heel) was dissolved in run SX-35 and 80% for run SX-37 which is approximately 10% less than for runs SX-31 and 33. This, of course, indicates an appreciable buildup in heel from one run to the next (2260 g for run SX-35 as compared to 2971 g for run SX-37).

At the conclusion of run SX-37 the residue was removed from the dissolver and segregated into 3 fractions: -20 mesh fines, UO_2-ThO_2 pellet fragments, and stainless steel and braze metal fragments (see Figure 7.2). The total weight of residue was 2058 g consisting of 329 g fines, 1686 g UO_2-ThO_2 fragments (3.6% of total weight of pellets charged), and 43 g of stainless steel and braze metal fragments (0.26% of total weight of stainless and braze). The fines consisted primarily of particles of stainless steel and braze metal and the carbonaceous material generated during the dissolution

UNCLASSIFIED
PHOTO 49576

Fines
(329 grams)

UO_2-ThO_2
Pellet Fragments
(1686 grams)

Stainless Steel and Braze
Metal Fragments
(43 grams)

Fig. 7.2. Dissolver residue at the conclusion of run SX-37.

of stainless steel in H_2SO_4. It should be noted that the actual weight of UO_2-ThO_2 heel was 1686 g as compared to the 2971 g estimated from analyses of core solutions. There was no visual evidence of an appreciable heel built up from one run to the next.

The total weight of residue was batch dissolved using a 300% excess of dissolvent (13 M HNO_3, 0.04 M fluoride, 0.1 M Al^{+++}). After approximately 23 hrs of refluxing, 178 g of residue consisting of 62 g fines, 100 g UO_2-ThO_2 fragments, and 16 g of stainless steel and braze metal fragment remained. The 100 g of UO_2-ThO_2 fragments represent approximately 0.02% of the total weight (46456 g) of UO_2-ThO_2 pellets charged to the dissolver.

7.3 Mechanical Processing - G. K. Ellis, J. B. Adams, G. A. West, G. B. Dinsmore

Shearing. The production prototype shear for use in the mechanical processing of spent irradiated fuel assemblies must produce essentially discrete single sheared pieces to provide a suitably sized feed for the continuous leachers. In tests, discrete pieces have been produced shearing the Mark I prototype, porcelain-filled fuel assembly except in the last 6-in. remaining end of the bundle (Unit Operations Section monthly report, September 1959). Shear blades shaped to rearrange the bundle cross-section generate forces during shearing that stress and fracture the brazed joint between tubes and ferrules and produce discrete single cylinders suitable as feed to a continuous leacher. It is uncertain, however, whether discrete pieces of sheared feed can be maintained when shearing assemblies fabricated by a new technique of brazing now being used to assemble Yankee and Nuclear Ship Savannah fuels.

Westinghouse Electric Corporation, after an extensive program,* has developed a brazing technique for fabricating the Yankee sub-assembly which it is reported, will more frequently tear at the ferrule walls than fracture the brazed joints when a wedge is driven between the tube layers. "By carefully controlling the amount of brazing alloy, joint clearances, brazing temperature and time at temperature, it is possible to produce 'diffusion bonded' joints which are as strong or stronger than the stainless steel base metal."** This is a stronger brazed joint than has been observed before and it results primarily from closer tolerances between fuel assembly tubes and ferrules. Good fit-up (joint clearance less than 0.002-in.) is maintained by a special jig design which compresses the bundle during the brazing in a vertical furnace. There is better fit-up of the assembly and placement of braze material using Kanigen nickel-phosphorus (7-10 per cent P) plated ferrules than using Nicrobraz 50 because of advantages inherent in the technique of braze application by Kanigen electroless plating. The electroless 0.001-in. thick plating on ferrules may be exactly controlled to ±0.0001-in. by varying the deposition time. Advantage may be taken, of a 3-hr time at brazing temperature (50 to 100°F above the brazing alloy melting temperature) to

* "Joining Fuel Rods Into Subassemblies for YAEC Fuel Elements," Westinghouse Electric Corporation, December 4, 1958.

** IBID, p. 30.

diffuse phosphorus out of the weld joint and alloy the base metal with braze metal with braze material in the joint, only if there is good fit-up between tubes and ferrules. Depletion of embrittling phosphorus from the joint during this long time at temperature is said to give the braze joint strength and ductility comparable to the base metal.

The effect on the mechanical processing program of ductile weld joints from this brazing technique must be evaluated in tests with Kanigen brazed fuel assembly sections. Surplus samples of representatively brazed Yankee sub-assembly sections have been requested for testing from Westinghouse.

The significant question introduced by this new brazing procedure is whether essentially discrete single sheared pieces will still be produced shearing with a stepped "M" shaped punch, the shape chosen for initial use in the production prototype shear being designed by Birdsboro Machine and Foundry Company. Failure to meet this requirement will require some redesign of the production prototype shear by Birdsboro. Tests must be made with the impact wedge (Unit Operations Section monthly report, March 1959) to re-evaluate the use of this device with more ductile braze joints. In earlier tests (Unit Operations Section monthly progress report, June 1959) it was not possible to disassemble a Consolidated Edison prototype fuel assembled with the ductile Coast Metals NP 50 braze by fracturing the braze joints using the same impact wedge which successfully disassembled the Consolidated Edison assembled with Nicrobraz 50. However, it should be observed that these Nicrobraz 50 joints might have been equally ductile and difficult to disassemble if there had been closer fit-up of assembly elements and longer times at brazing temperature.

Leaching. Effective surface area measurements of partially dissolved UO_2 pellets in conjunction with existing dissolution rate data of whole pellets in nitric acid will allow calculation of operating characteristics of various types of dissolvers and leachers. A comparison of the relative effectiveness of various types of large equipment could be made without building and operating each type.

The effective area of unirradiated UO_2 pellets dissolving in nitric acid was determined as a function of the fraction dissolved. The effective area was estimated relative to the superficial surface area of a fresh pellet (right cylinder, $L_o \cong D_o \cong 0.417$-in.). The relative area was calculated using the rate of weight loss of partially dissolved pellets and the rate of dissolution of fresh pellets taken over a short period. After a short dissolution period fresh pellets became porous, the effective area becoming 3 to 5 times the initial area. The results were quite variable (Figure 7.3). The data was fitted approximately by the relation:

$$\frac{A}{A_o} = 1 + 47\left(1 - \frac{W}{W_o}\right)^2 - 92\left(1 - \frac{W}{W_o}\right)^3 + 44\left(1 - \frac{W}{W_o}\right)^4 \quad *$$

* See nomenclature

UNCLASSIFIED
ORNL-LR-DWG 48491

Conditions: UO_2 Pellets
D_o = 0.417 in.
L_o = 0.417 in.
W_o = 9.65 g. A_o = 5.29 cm^2
7 *M* HNO_3, Boiling

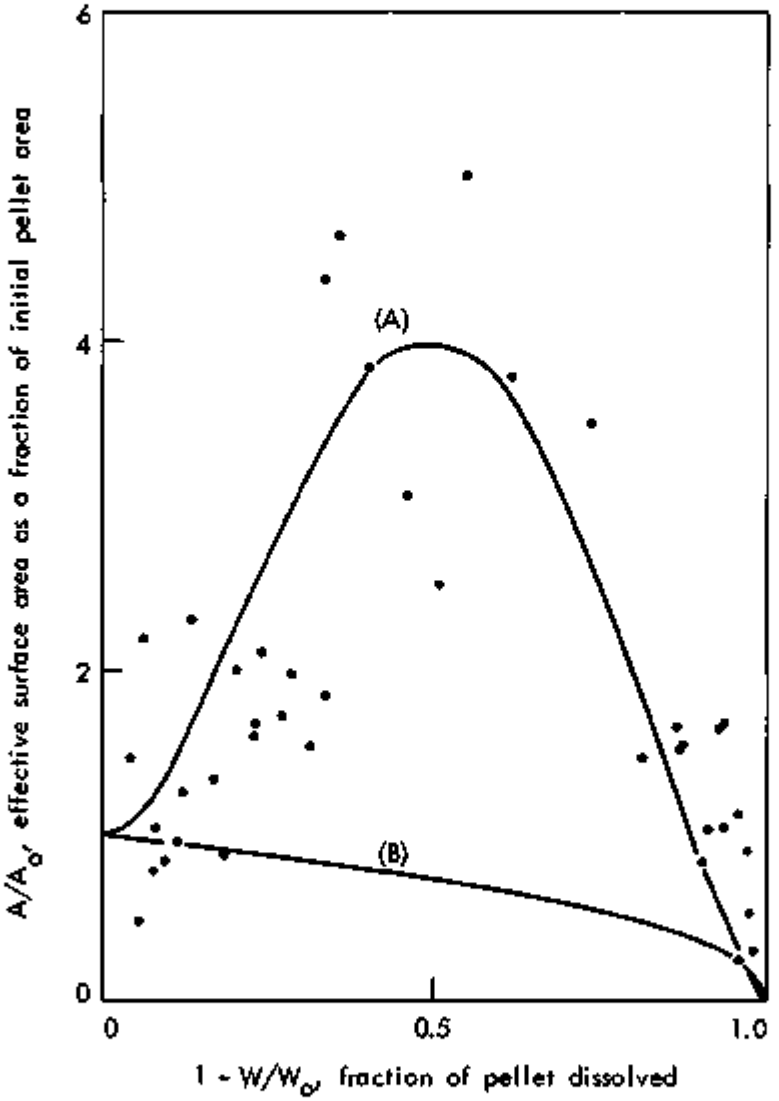

Curves: (A) $A/A_o = 1 + 47\ (1 - W/W_o)^2 - 92\ (1 - W/W_o)^3 + 44\ (1 - W/W_o)^4$

(B) $A/A_o = (W/W_o)^{2/3}$

Fig. 7.3. Effective surface area of UO_2 pellets dissolving in nitric acid.

The present data scatter by more than a factor of two in many instances which hardly justifies the effort to attempt a better fit.* Similar data may be derived from study of batch dissolution to completion of pellets in a large excess of dissolvent (so that its composition changes only slightly over the complete dissolution). Such data should be in a more useful form and more directly applicable to reactor design when used in conjunction with existing rate data** on initial pellets.

An estimate of the area per unit weight-vs-weight can be obtained for pellets with a well developed porous structure which occurred in the present set of data, after more than ~35% of a pellet was dissolved. This is plotted in Figure 7.4 and is applicable in general for fragments of UO_2 pellets small enough ($\lesssim$ 6 g) that they could be presumed to have come from a pellet of the size used. An extrapolation to heavier pellet fragments should be valid at least over a short range. This data does not apply in general to larger pellets, and probably not to odd shapes--long rods or flat discs--where a high degree of porosity may develop more rapidly.

Data was taken by exposing batches of partially dissolved pellets to boiling 7 M nitric acid for 2 min periods then quenching the reaction by dipping the pellets first in cold water then in acetone. Pellets were weighed individually before and after each run and were supported individually on a coarse mesh wire basket during dissolution. The rate of dissolution of fresh pellets was estimated as 30 $mg\text{-}cm^{-2}\text{-}min^{-1}$ from previous data** and from checks in the present series of data. Representative fresh pellets from the batch used had the following properties:

Length	0.417-in. ($\pm$ 0.013-in.)
Diameter	0.417-in. ($\pm$ 0.002-in.)
Weight	9.65 g ($\pm$ 0.14 g)
Surface Area	5.29 sq cm ($\pm$ 0.13 sq cm)

with approximate variability as indicated.

There are several limitations on the application of the results. The method used assumes uniform density throughout the pellet structure which is not true. The results apply strictly to the type of pellets tested. It appears, however, that it may be a useful representation for pellets of the same density (10.1 - 10.4 g/cc), nearly the same size and with only a moderate

* Although the application of refinements in curve fitting to data of such inherent variability is doubtful, use of equation fitted represents the actual situation more realistically than assuming the effective area to be the superficial surface exposed as a pellet dissolves at an equal rate into all surfaces. This approach ignors development of increased porosity and results in the equation $A/A_o = (1 - W/W_o)^{2/3}$ which is far out of line with experimental results as expected.

** TID-7583

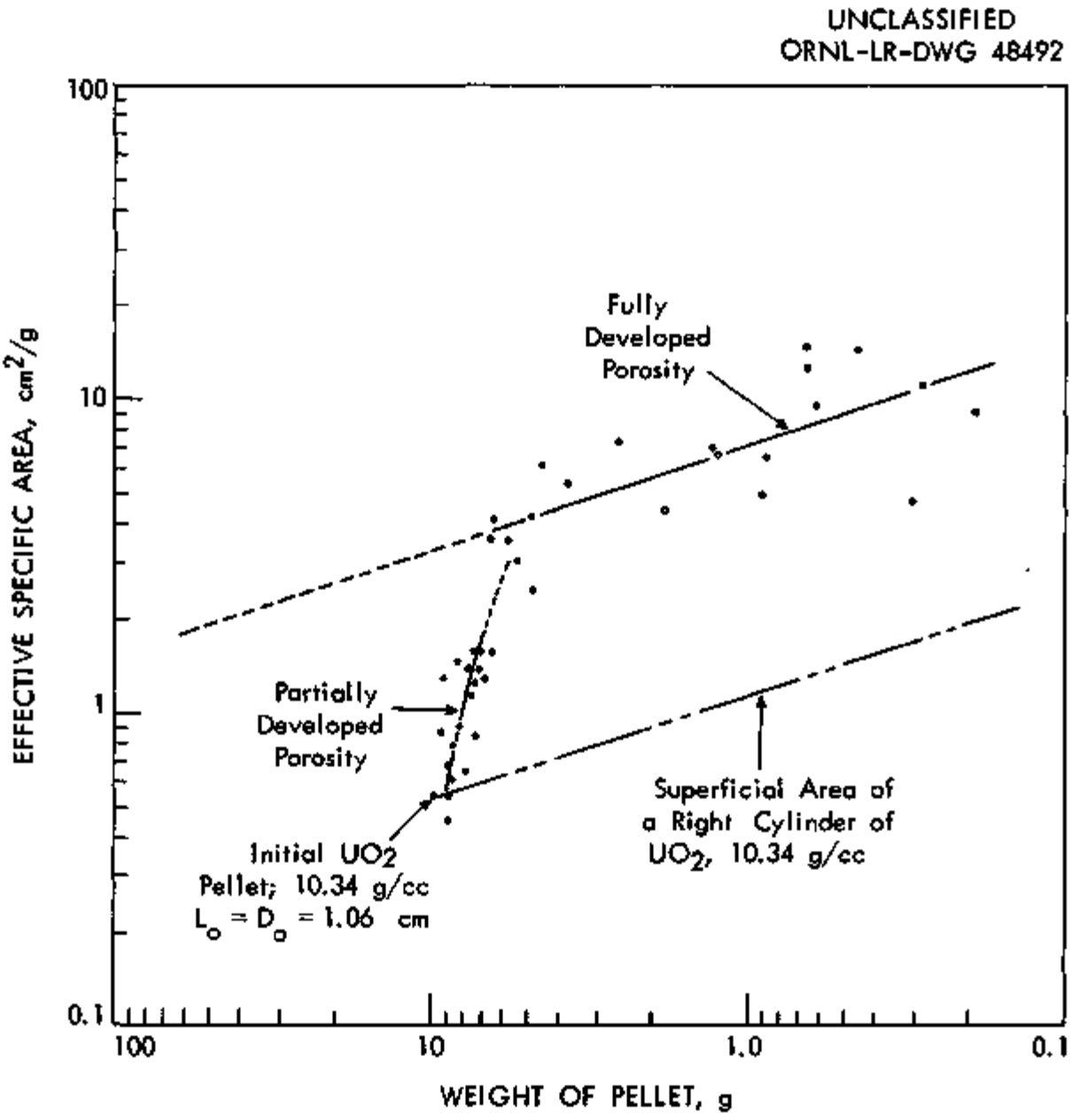

Fig. 7.4. Estimated effective specific surface area of UO_2 pellets dissolving in nitric acid.

variation in diameter and diameter-to-length ratio. In addition, only one dissolvent strength--7 M nitric acid--was used (to obtain a small enough dissolution rate that pellets would change in size and weight only moderately). It is possible somewhat different results would be obtained using stronger dissolvents which could produce dissolution rates up to 8 times as rapid.**

Nomenclature (consistent units)

A = effective area of pellet during dissolution

A_o = superficial surface area of a fresh pellet

W = weight of a partially dissolved pellet

W_o = weight of a fresh pellet

SRE Dejacketing Studies. The mechanical equipment installed in the High Level Segmenting Facility to demonstrate the dejacketing of stainless steel jacketed-NaK bonded-uranium fuel rods of the SRE, Core I, has continued to operate satisfactorily during repeated mechanical operability tests. A few alignment and tolerance corrections were necessary for optimum operation of the hydraulic dejacketing machine, especially the alignment and clearance of the guide nut and pressure screw within the collet mechanism.

A single performance test of hydraulically expanding 10 mil thick wall, SRE prototype, stainless steel tubing indicated that the tubing would start expanding at 800 psig and expand about 45 mils in 30 seconds at 1300 psig. The hydraulic pressure is supplied by a Oil Dyne pump which pumps No. 6 white mineral oil from the dejacketer tank and into the tubing. The same unit is used to flush the slugs out of the tubing after the expansion procedure and the end plug removal. Cambered steel slugs were flushed out of the tubing at approximately 100 psig pressure. A pressure of only 200 psig supplied to the collet mechanism is sufficient clamping and holding force on the tube to restrain it while it is being expanded.

The long (~9 ft) pressure screw in the dejacketing machine is driven by a 2 speed, reversible electric motor with a mechanical clutch. The clutch required adjusting so that no more than 700 pounds force could be applied on the screw threads. A special device with a pressure indicating gauge was used in the tests for accurately setting the clutch tension.

The auxiliary dejacketing die did not satisfactorily slit the 6-in. lengths of cladding in repeated tests. Alterations to the die did not improve its performance sufficiently to warrant additional tests on the unit. A new unit incorporating a different design concept is being fabricated which employs rollers preceeding the cutting tools to score the tube wall thus alleviating the work load on the cutters.

The hydraulic multipurpose saw was operated in the effort to locate and correct excessive vibration and noise created by the Vickers hydraulic

** TID-7583

system. The Vickers Company supplied additional flow and check valves which are being installed to help reduce the noise level. The saw movements, both vertical and horizontal and its rotation on the spindle, have operated reasonably well but better control of vertical travel is needed. Additional tests are to be made on the method of changing blades and securing the blade on the spindle before final approval is made.

8.0 SOLVENT EXTRACTION STUDIES

A. D. Ryon

Flooding values reported this month were obtained using the acid Thorex flowsheet. The experimental techniques and a description of the columns may be found in the October monthly report (CF 59-10-77).

8.1 Pulse Column Performance Studies - R. S. Lowrie, F. L. Daley

Work was started this month to evaluate the flow capacity and stage efficiency of pulse columns as a function of operating variables and cartridge design for the acid Thorex flowsheet developed by Chemical Development Section B.* This flowsheet, intended for the Consolidated Edison fuels, utilized a feed ≅ 0.1 M acid difficient, a dual scrub and the addition of salting acid near the bottom of the extraction section. The stripping agent was ≅ 0.01 M aluminum nitrate solution. The experimental conditions for this flowsheet are shown in Table 8.1. Figure 8.1 is a schematic diagram showing where the various streams were introduced into or taken from the compound extraction scrub columns.

The flooding rates obtained this month are shown in Table 8.2. The sieve plate extraction column flooded at 1030 GSFH when operated aqueous continuous and at 1690 GSFH when operated organic continuous (pulse frequency = 50 cpm). The flow capacity of the nozzle plate extraction column increased from 500 to 1400 GSFH as the pulse frequency decreased from 70 to 30 cpm. Flooding occurred in the 12-ft sieve plate stripping columns at 1290 GSFH, for both aqueous and organic continuous operation at 35-cpm pulse frequency. Flooding capacity in the 12-ft nozzle plate stripping column (0.188-in.-dia hole, 23% free area) was increased from 2080 GSFH to 2280 by changing from aqueous-continuous to organic-continuous operation at 35 cpm pulse frequency. Assuming that the pilot plant would process 120-kg thorium per day, the flow rate would be 375 GSFH for the extraction column and 700 GSFH for the stripping columns which are well below the flooding rates reported. However, the ultimate capacity would be limited by the capacity of the strip column.

---

* Chemical Technology Division Chemical Development Section B Monthly Progress Report December 1959, pp 19-21, ORNL CF 59-12-74.

Table 8.1. Experimental Conditions - Acid Thorex Flowsheet

Stream	Relative Flow	Uranium, g/liter	Thorium, g/liter	HNO_3, M	Other
Feed	100	20.0	250	0.10 AD	F = 1.0 g/liter SO_4 = 0.8 g/liter Al = 1.09 g/liter
AS_1 scrub	80	-	-	-	Water scrub
AS_2 scrub	20	-	-	5.0	---
14 MA scrub	50	-	-	14.0	Technical grade conc. HNO_3
AX solvent	700	-	-	-	30% TBP in Amsco 125-82 diluent
CX strip	1050	-	-	-	0.01 M $Al(NO_3)_3$ sol'n

Table 8.2. Flooding Rates - Acid Thorex Flowsheet

Pulse Frequency, cpm	Phase Cont.	Cartridge	Flooding Rate at Bottom of Column - GSFH
Extraction Column			
50	aqueous	sieve plate	1030
50	organic	sieve plate	1690
30	organic	0.125-in. nozzle plate	1400
50	organic	0.125-in. nozzle plate	1250
70	organic	0.125-in. nozzle plate	500
Stripping Column			
35	aqueous	sieve plate	1290
35	organic	sieve plate	1290
35	aqueous	0.188-in. nozzle plate	2080
35	organic	0.188-in. nozzle plate	2280

Pulse amplitude = 1 inch

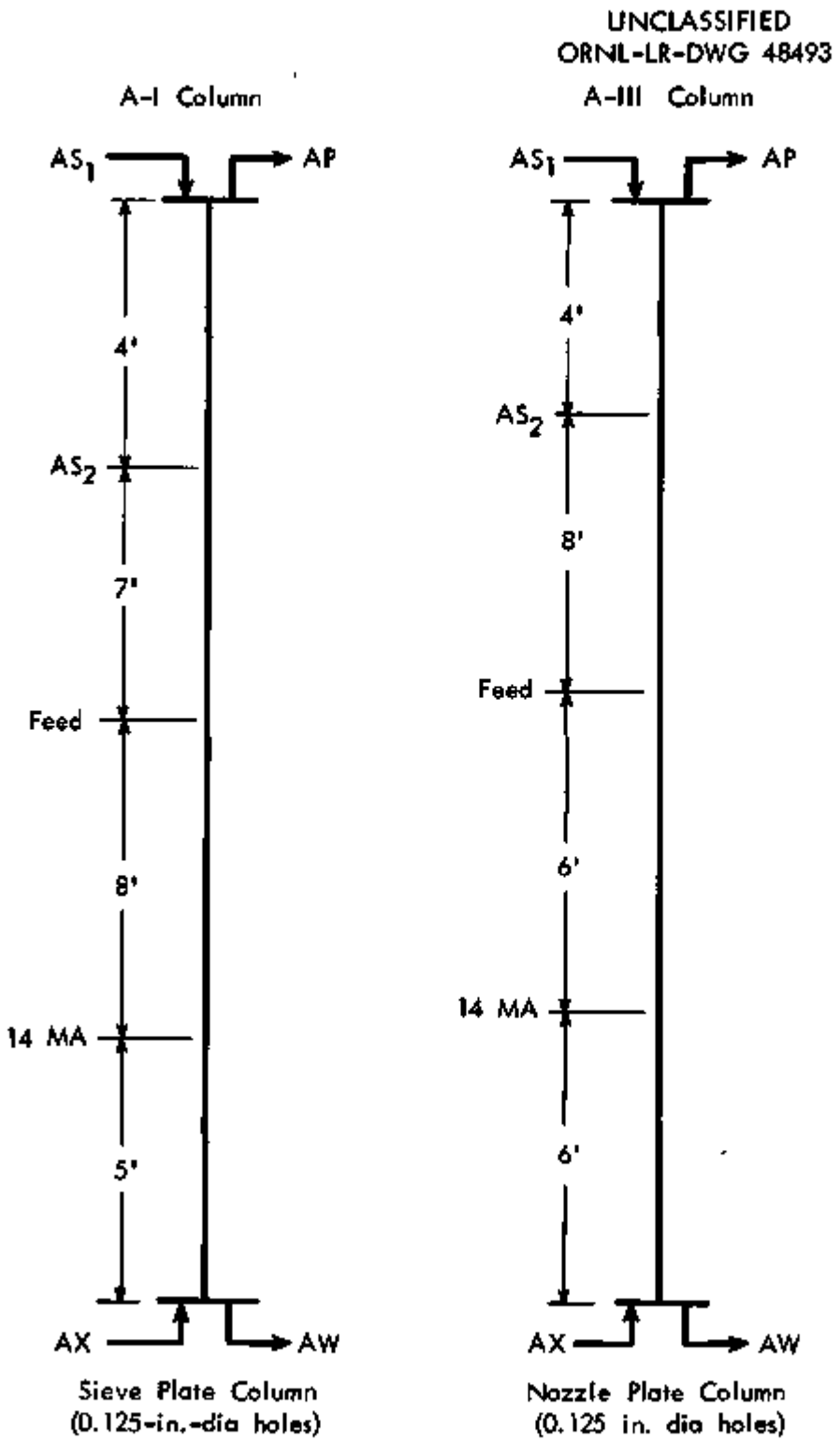

Fig. 8.1. Compound extraction-scrub columns for the acid Thorex flowsheet.

9.0 VOLATILITY

R. W. Horton

9.1 UF_6 Stream Analysis - L. E. McNeese

A Condensation Pressure Analyzer has been installed for continuous analysis for UF_6 in inert streams (N_2, A, F_2, or mixtures) from experimental systems. The principle of operation is that of measurement of the total pressure required for condensation equilibrium between the sample gas and a condensed component in a constant temperature capillary (equilibrium condensation pressure). The work reported here deals with the design of a constant temperature bath and its testing at 0°C and -22.8°C.

Design of Cold Batch. A constant temperature batch exploiting the sharp volume change of a freezing liquid was designed as suggested by W. S. Pappas and C. W. Weber (Figure 9.1). The cold bath was designed to be completely filled with a liquid having a freezing point equal the desired bath temperature. Cooling coils at the top were provided for circulation of chilled trichloroethylene at ~ -40°C. The volumetric change of the system upon partial freezing was detected by a microswitch actuated by a 1-in. dia bellows. The signal from the microswitch controlled a solenoid valve in the coolant line so that ice would be present at all times. A magnetic stirrer in the cold bath maintained equilibrium between the liquid and solid phases. Two capillaries, (1/8-in. and 3/16-in. dia) were inserted in the lower part of the bath.

Survey of Possible Bath Liquids. The UF_6 concentration in a gas sample is related to the equilibrium partial pressure as

$$P = \frac{p}{Y}$$

where P = equilibrium condensation pressure, p = UF_6 vapor pressure, Y = UF_6 mol fraction so that at a given temperature the equilibrium condensation pressure may range from the vapor pressure of UF_6 to ∞. It is desirable to maintain the equilibrium condensation pressure in the range 0-825 mm Hg absolute so as to not restrict the sample pressure unduly.

As shown in Figure 9.2, using H_2O as the bath liquid, the minimum detectable UF_6 concentration is 2.1 mol %. Using CCl_4 however, 0.3 mol % UF_6 can be detected. It should be noted, however, that when CCl_4 is used the average signal in the UF_6 concentration range 40-100 mol % is only 0.06 mm Hg/mol percent which is much too small for accurate analysis. In the concentration range 0.3-20 mol %, a satisfactory average signal of 4.2 mm/mol percent is obtained. Thus, the signal may be improved in range of interest by selection of proper bath temperature. As well as having the proper freezing point, the bath material should also have a large change in volume on fusion in order to facilitate temperature control. Properties of several possible bath materials are shown in Table 9.1. Shown also is the concentration range of practical interest over which the minimum signal is 0.5 mm Hg/mol percent UF_6.

UNCLASSIFIED
ORNL-LR-DWG 48494

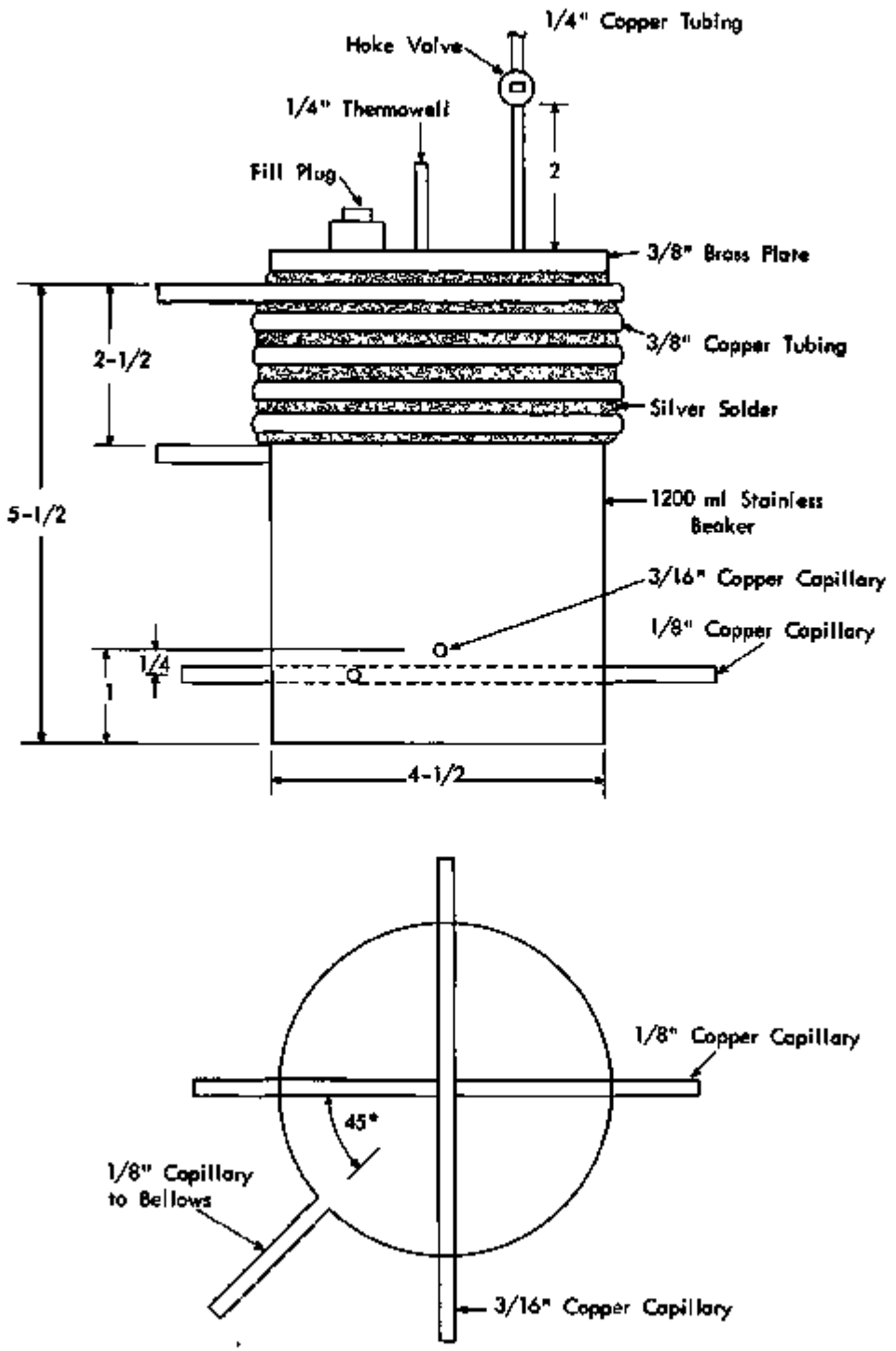

Fig. 9.1. Cold bath assembly.

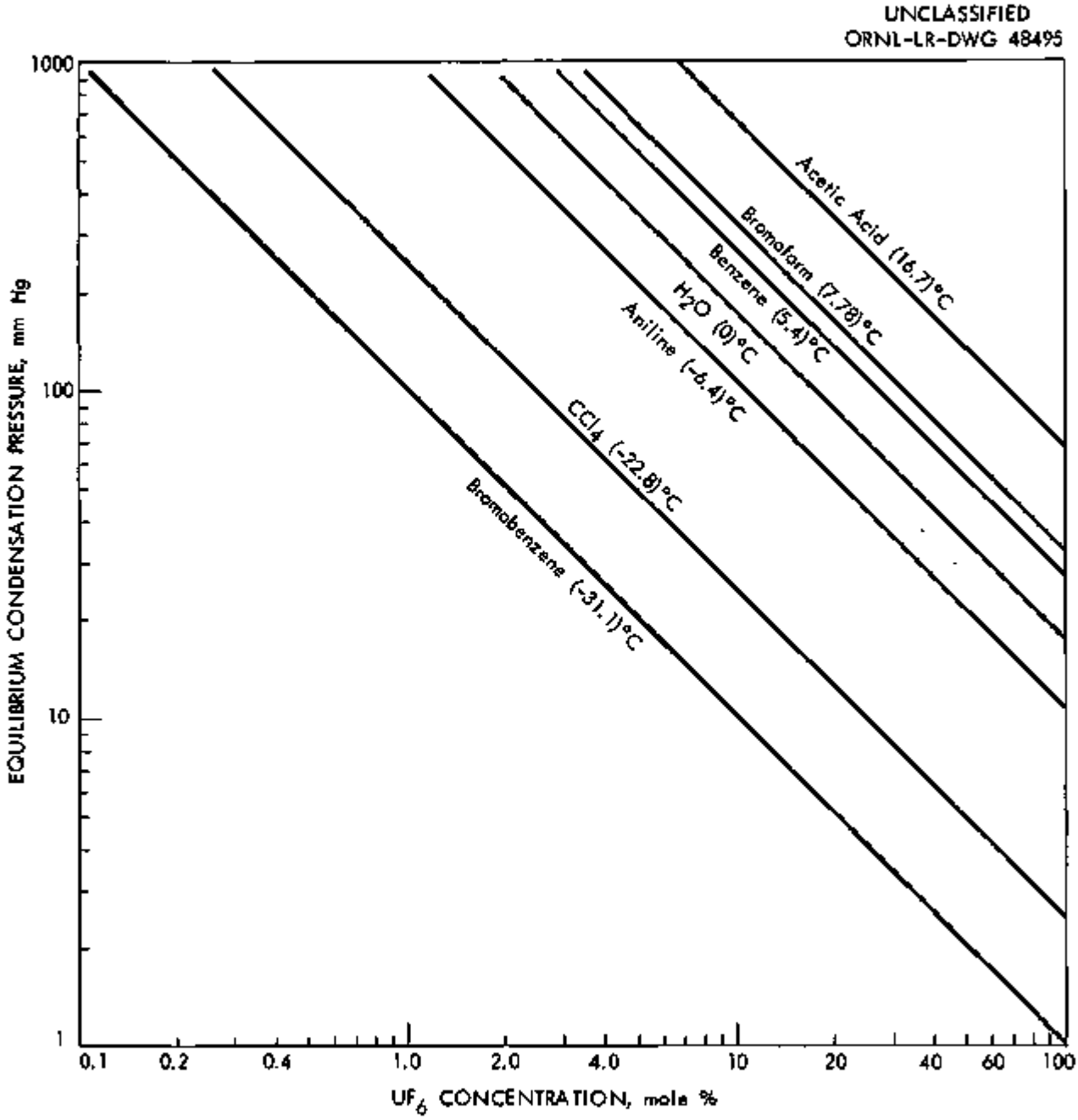

Fig. 9.2. Equilibrium condensation pressure for various liquids.

Table 9.1. Characteristics of Possible Bath Materials

Freezing Point °C	Bath Material	Change in Volume on fusion $cm^3/100$ kg	UF_6 Vapor Pressure mm Hg	Concentration Range mol % UF_6	
				*Minimum	+Practical
16.68	$C_2H_4O_2$	-156	67.2	8.0	8.0 - 100
7.78	$CHBr_3$	- 39.1	32.6	3.95	4 - 90
5.4	C_6H_6	-131.7	27.4	3.5	3.5 - 85
0	H_2O	90.0	17.57	2.13	2.1 - 70
- 6.4	C_6H_7N	- 85.4	10.85	1.3	1.3 - 60
- 22.6	CCl_4	-25.8	2.48	0.3	0.3 - 30
- 31.1	C_6H_5Br	~ -55	1.034	0.125	0.13 - 20

* Based on maximum equilibrium condensation pressure = 825 mm Hg.

\+ Based on minimum response of 0.5 mm Hg/mol percent UF_6.

It should be noted that as the UF_6 concentration is decreased, the response time for the instrument will be increased so that the mere existence of the proper temperature for detection of 0.1 mol % UF_6 does not guarantee proper operation of the analyzer at this concentration.

Experimental Results. The experimentally observed temperature variations in bath temperature using H_2O and CCl_4 were $< \pm 0.01°C$ and $\pm 0.2°C$, respectively. It is probable that air in the system during the test with CCl_4 contributed to poor control, as did the relatively small volume change on fusion. It is believed that either system will yield an acceptably constant temperature.

9.2 Moving Bed Absorber - R. J. McNamee, V. R. Young, Z. R. McNutt

Preliminary testing of a sodium fluoride pellet movable bed unit which would serve as both an absorber and CRP trap in the Volatility Pilot Plant is being carried out. Following the mechanical operability tests (reported last month), four runs were made in which hydrogen fluoride gas was passed through the bed to simulate sorption conditions in process operation (Table 9.2). The purpose of these tests was to determine the sorption location pattern in the bed as a function of time and gas flow rate. Since caking in the vertical section of the bed results in failure of the pellets to fall by gravity, the CRP sorption should all take place in the horizontal section of the bed. Run 1 indicated that even a small amount of HF in the vertical bed can cause trouble. Sorption data are necessary in order to estimate the length of horizontal bed required for a given length run (before discharge) or conversely the required frequency of discharge for a given length bed, in order to prevent break-through into the vertical section.

The horizontal section of the bed was loaded to 88% of calculated capacity with HF running for 6 hr, at rates up to 0.9 lb/hr. The hydraulic pressure on the piston drive to discharge the loaded bed increased from 40 to 140 psig; solidly caked pellets were discharged. Under these loading conditions only 60% of the HF added sorbed on the horizontal bed. The pattern of bed loading was clearly defined by sharp temperature increases (indicated by a thermocouple array) which resulted from sorption of concentrated HF on the pellets. Further tests with dilute HF streams will be required to determine the loading at and time for break-through into the vertical section for a range of flow rates.

In an attempt to determine the amount of HF sorbed in various sections of the bed, pellet samples were taken and leached with water, which was then titrated. However, the method was unsuccessful due to the extremely slow leaching rate.

Prior to run 3, five thermocouples were inserted into the horizontal bed as shown in Figure 9.3. Their purpose was to indicate the sorption pattern in the horizontal bed by means of the temperature rise (due to heat of sorption) sequence of the five points. This sorption sequence is given on Figure 9.3 by the consecutive numbers. The results are given in Table 9.3.

Table 9.2. Summary - HF Sorption Runs

Conditions: Room temperature
HF concentration ~100%

Run No.	HF Fed lb	Duration hr	Type of Bed[a]	Wt % HF Which Sorbed in Horizontal Bed[e]	Maximum Bed Discharge Pressure[b] psig	Remarks
1	1.9	1/2	Partial	~100	140	Pellets stuck in vertical section upon discharge.
2	0.2	1/6	Partial	-	49	No vertical section sticking.
3	1.1	2	Filled			
4[c]	3.6	4	Filled	60	140[d]	Pellets stuck in vertical section upon discharge. All pellets discharged. All batches showed some caking.

(a) Partial bed formed by single retraction of piston, as contrasted to "Filled" bed, as discussed in last month's report.
(b) Normal pressure ~40 psig.
(c) No pellet discharge after run 3. Data represents HF accumulation during both runs.
(d) Severe caking in horizontal section. One solid chunk weighed 1-3/4 lb.
(e) Calculated from bed weight gain.

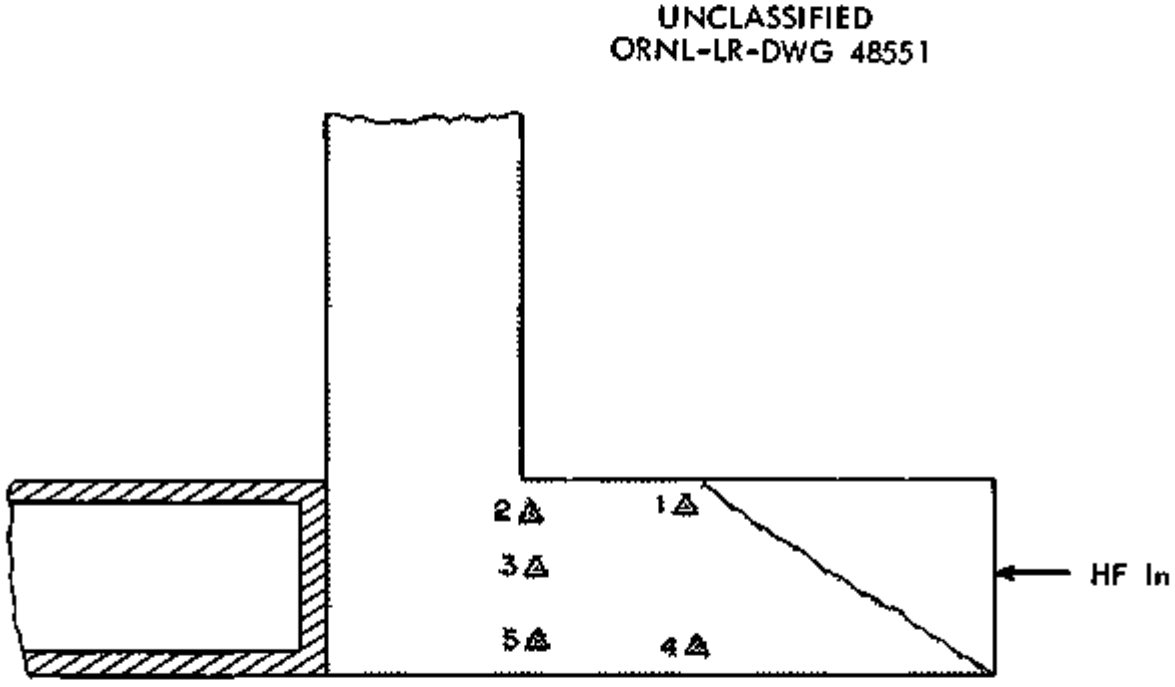

Fig. 9.3. Thermocouple locations, indicating the HF sorption sequence in the horizontal bed.

Table 9.3. Indication of HF Sorption Location as a Function of Time

Conditions: Data taken on runs 3 and 4, using same bed (thermocouples located as shown in Figure 9.3).
Bed cooled overnight between runs.
HF Rate: run 3 - 0.5 lb/hr
run 4 - 0.9 lb/hr
Bed Dia. - 5-in.

Time hr-min	Temperature and Rate of Change of Temperature[a] °C and °C/min										Temperature on External Surface of Vertical Pipe, 10-in. Up Bed
	T.C. 1		T.C. 2		T.C. 3		T.C. 4		T.C. 5		
0-1	20		20		20		20		20		
0-8	55	5.00	30	1.43							
0-15	98	6.14	45	2.14							
0-23	137	4.88	73	3.50							
0-31	140	0.38	60	1.00							
0-45	141	0.07	95	0.27	30	1.47	25	0.67	22	0.33	
1-0	138		99	0.35	52	2.12	35	1.00	27	0.47	
1-17	133		105	0.54	88	2.62	52	1.69	35	0.41	
1-30	130		112	0.33	122	2.53	74	1.13	42	0.67	
1-45	125		117	0.33	160	2.27	91	0.60	52	0.87	
2-0	120		122		194		100		65		
	Start run 4										
0-0	27										
0-6	43	2.67									
0-20	65	1.57	35								
0-30	69	0.40	43	0.80							
0-35	69	0.0	47	0.80							
0-45	72	0.30	52	0.50							
1-0	75	0.20	62	0.67	30	1.40	27	2.53			
1-8	75	0.0	66	0.50	51	3.00	65	4.25	30	0.62	20
1-15	75	0.0	70	0.57	75	8.14	99	1.00	35	0.71	
1-25	75	0.0	75	0.50	132	7.30	106	0.20	40	1.00	21
1-35			81	0.60	205	3.40	108	0.0	50	1.80	
1-50			95	0.93	239	0.73	108	0.27	68	3.47	24
2-7			105	0.59	250	0.12	112		120	2.47	27
2-30		0.10	113	0.35	252	0.0	110		162	1.70	
2-45			120	0.47	252		100		201		37
3-0			125	0.33	252				194		
3-15	86		127	0.13	251		75		179		52
3-30	86	0.0	130	0.20	251		70		173		55
3-45	84		133	0.20	250		65		170		62
4-0	82		133	0.0	248		60		165		68
									161		75

(a) Assumed proportional to sorption rate.

In run 3, the initial sorption rate was by far the highest at location 1, but also noticeable at location 2. However, these dropped off rapidly. Sorption did not become evident at sites 3, 4, and 5 until after 45 min, with site 3 predominating.

In run 4, initial sorption again took place at site 1, but it rapidly decreased to essentially none after 30 min. Sorption then principally took place at sites 4, 3, and 5 (in that order). For the last 1-1/2 hr of the run, little further sorption could be detected.

Sixty percent of the HF introduced during runs 3 and 4 was sorbed in the horizontal bed; the bed was 88% saturated, based on the formation of the NaF-HF complex (in general, the resulting bed temperature was too high to allow higher HF content complexes). The temperature rise data reflect the decreasing sorption rate (mols HF sorbed/(mol NaF)(min)) as the bed loading increases. Since the HF input rate was constant, the amount passing (not sorbed) any site increased with time. There was an indication of sorption 10-in. up the vertical bed after only 1-1/2 hr of run 4. This temperature rise became much greater after the horizontal bed sorption essentially ceased (38°C over the remaining 1-1/2 hr of run 4, 17°C in the 2-1/2 hr prior to this), showing that the principal sorption was then in the vertical region.

The sorption (temperature rise) data indicate that the least sorption took place at sites 4 and 5, probably due to the fact that this portion of the bed would have the greatest resistance to gas flow.

10.0 WASTE PROCESSING

J. C. Suddath

The objective of the waste processing program is to obtain the engineering data required for the design of a plant for reducing high-activity liquid waste to solids for permanent disposal. During this period, work progressed on (1) pot calcination of simulated waste, (2) aerosol attenuation in a packed distillation tower and (3) remote handling of calcination vessels.

10.1 Pot Calcination - C. W. Hancher

Test R-29 (Purex pot calcination) has been completed. All of the equipment operated without malfunction. The pot was filled with boiling water before the test was started. The results will be presented in detail next month. The preliminary results are as follows:

Overall feed volume - 435 liters

Average feed rate - 9.2 liters/hr

Total solids in pot - 89 kg

Average density of solids - 1.37 g/cu cm

10.2 Particulate Attenuation in a Packed Distillation Tower - J. J. Perona

The effectiveness of a distillation tower as an aerosol attenuator is being studied as a function of tower operating variables and aerosol properties. A series of runs was made in which an air stream bearing an aerosol of $Cr(NO_3)_3 \cdot 9H_2O$ containing Cr-51 tracer was fed into the bottom of a packed distillation tower operating with water at total reflux. The activity in the exit air stream was reduced to essentially background over the range of vapor compositions studied of 0.30 to 0.95 mol fraction steam. The volumetric average diameter of the aerosol, $\Sigma nd^3/\Sigma n$, was in the range of 10 to 15μ. Experiments without steam in the tower showed that particle growth was necessary for good decontamination of the air stream.

Four runs were made in which water (at about 60°C) was fed into the top of the tower and the air stream was passed up through the tower, with no steam generated by the reboiler. In three of the runs, decontamination factors below 10 were obtained, showing that particle growth is necessary for good decontamination of the air stream (see Table 10.1). The fourth run, which was at the lowest air rate of the series, gave a decontamination factor of 1.8×10^3. The results of this run might be explained by the higher residence time of the aerosols in the tower, which would have permitted more particle growth. The argument that the higher water rate in this run may have resulted in better gas-liquid contacting does not appear to be tenable, since liquid rates as low as 74 lb/hr-sq ft were used in the series of runs with steam in the vapor phase.

Table 10.1. Particulate Attenuation in a Packed Scrubbing Tower

Air Stream Activities

Run No.	Air Rate, ft^3/min	Water Rate, $lb/hr\text{-}ft^2$	Activity of Air Stream counts/min-ft^3 In	Out	Decontamination Factor
16	0.22	233.	1.1×10^4	6.2	1.8×10^3
18	0.92	195	2.3×10^4	4.3×10^3	5.4
17	1.59	157	1.3×10^4	1.7×10^3	7.8
19	1.59	157	2.4×10^4	3.2×10^3	7.5

Liquid Stream Activities

Run No.	Average Activity, counts/min-cc Top of Tower	Top Third	Bottom Third	Bottom (Effluent)	Acid Wash	Length of Run, hr
16	0	1	0	34	1,131	6
18	22	4640	5320	531	12,950	6
17	2	925	61	114	5,470	6
19	39	704	745	1229	3,810	4

Samples of the liquid phase flowing down the tower were collected each hour at four points: (1) just below the top of the tower, (2) a third of the way down from the top, (3) two-thirds of the way down, and (4) at the bottom of the tower (Table 10.1). In runs 17 and 18 higher liquid phase activities occurred in the tower than in the liquid stream leaving the bottom of the tower. This peculiar effect was caused by higher particulate attenuation in the upper part of the tower, due to the higher temperature there which promoted particle growth, followed by plating out of some of the activity in the liquid phase onto the tower packing in the lower parts of the tower. By refluxing nitric acid in the tower at the end of each run and counting acid samples, it was found that the amounts of activity absorbed on the packing was of the same order as that carried out by the effluent.

10.3 Remote Connection and Disconnection of Calciner Pot in Calciner Cell - C. W. Hancher

One of the important handling problems to be solved on waste pot calcination is the remote connection, disconnection, and removal of the filled pot from the calcining cell. A waste pilot plant might have four cells: feed evaporation and make-up, calcination, off-gas treatment, and pot sealing, inspection and shipment.

This discussion will only cover the development of the operation of the calcination cell. As conceived, the calcination cell would be equipped with the following items:

1. Two remote flange bolting tools.
2. One pair manipulators (slaves) per tool area.
3. Top loading access port.
4. Overhead crane in suitable enclosure with a lifting capacity large enough to handle calciner pot shipping carriers.
5. Equipped for underwater maintenance.

The calciner pot will be connected, disconnected, removed, etc. by direct remote tools. However, major maintenance like furnace replacement will be done underwater if the cell can not be remotely decontaminated for direct maintenance.

The conceptual layout of the calcination cell has the following features to allow for the insertion and removal of the calciner pot (Figure 10.1).

1. An entry plug to accommodate the calciner pot.
2. A tool to remove the blank flange (blank flange used to lower clean pot and to seal filled pot).
3. A tool to connect pot to feed flange.

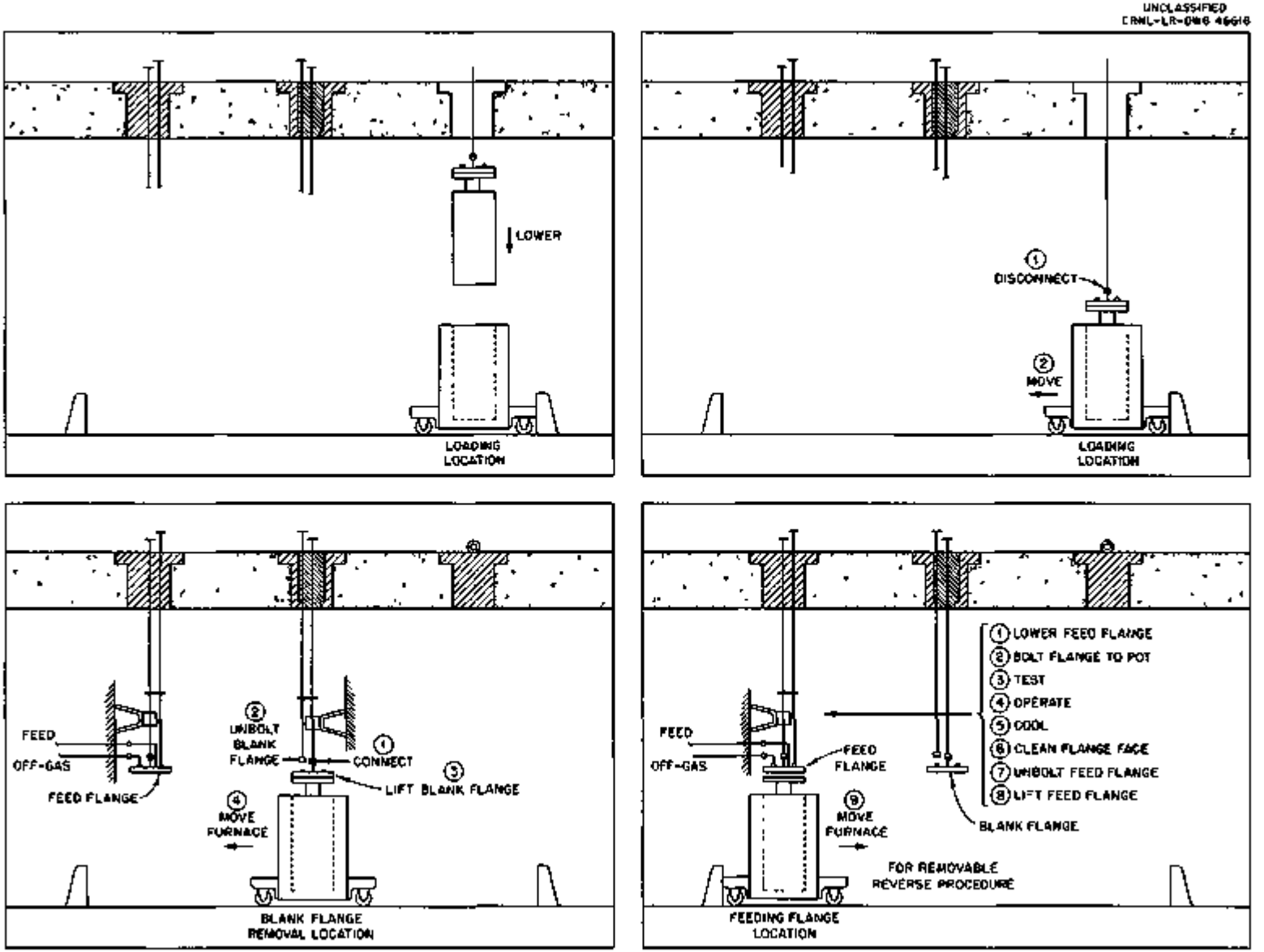
UNCLASSIFIED
ORNL-LR-DWG 46616
LOWER
LOADING LOCATION
1 DISCONNECT
2 MOVE
LOADING LOCATION
FEED
OFF-GAS
FEED FLANGE
2 UNBOLT BLANK FLANGE
1 CONNECT
3 LIFT BLANK FLANGE
4 MOVE FURNACE
BLANK FLANGE REMOVAL LOCATION
1 LOWER FEED FLANGE
2 BOLT FLANGE TO POT
3 TEST
4 OPERATE
5 COOL
6 CLEAN FLANGE FACE
7 UNBOLT FEED FLANGE
8 LIFT FEED FLANGE
FEED
OFF-GAS
FEED FLANGE
9 MOVE FURNACE
BLANK FLANGE
FOR REMOVABLE REVERSE PROCEDURE
FEEDING FLANGE LOCATION

FIG. 10.1

The tools for the blank flange removal and the feed flange (Figure 10.2) are the same, so that they can be interchanged. They consist of long-handled socket wrench (Figure 10.3) which rotates to the position of the four bolts of the 3-in. (No. 150) stainless steel flanges used for both.

A systematic study of the sealing variables has been started, the following variables will be studied:

1. Flange faces
2. Glaskets (stainless steel)
3. Bolts
4. Nuts
5. Gasket lubricant
6. Bolts lubricant

The new calciner pot will be equipped with new gaskets, a blank flange, and nuts, so these items will only be used twice including final storage. The feed flange and bolts will be reused. The bolts can be easily removed by leaving a bolt attached to the collect socket wrench and removing the tool.

A metal hood with separate off-gas line will be installed around the feed flange when the filled pot is to be open so that any contaminated dust involved will not contaminate the balance of the cell.

After the filled pot has been sealed with a blank flange it is moved to the final sealing and inspection cell where a seal bonnet (Figure 10.4) is placed on the flange and welded to pot, making welded seal. Then the exterior of the pot is decontaminated for shipping. The pot can be loaded into a bottom loading carrier from the inspection cell.

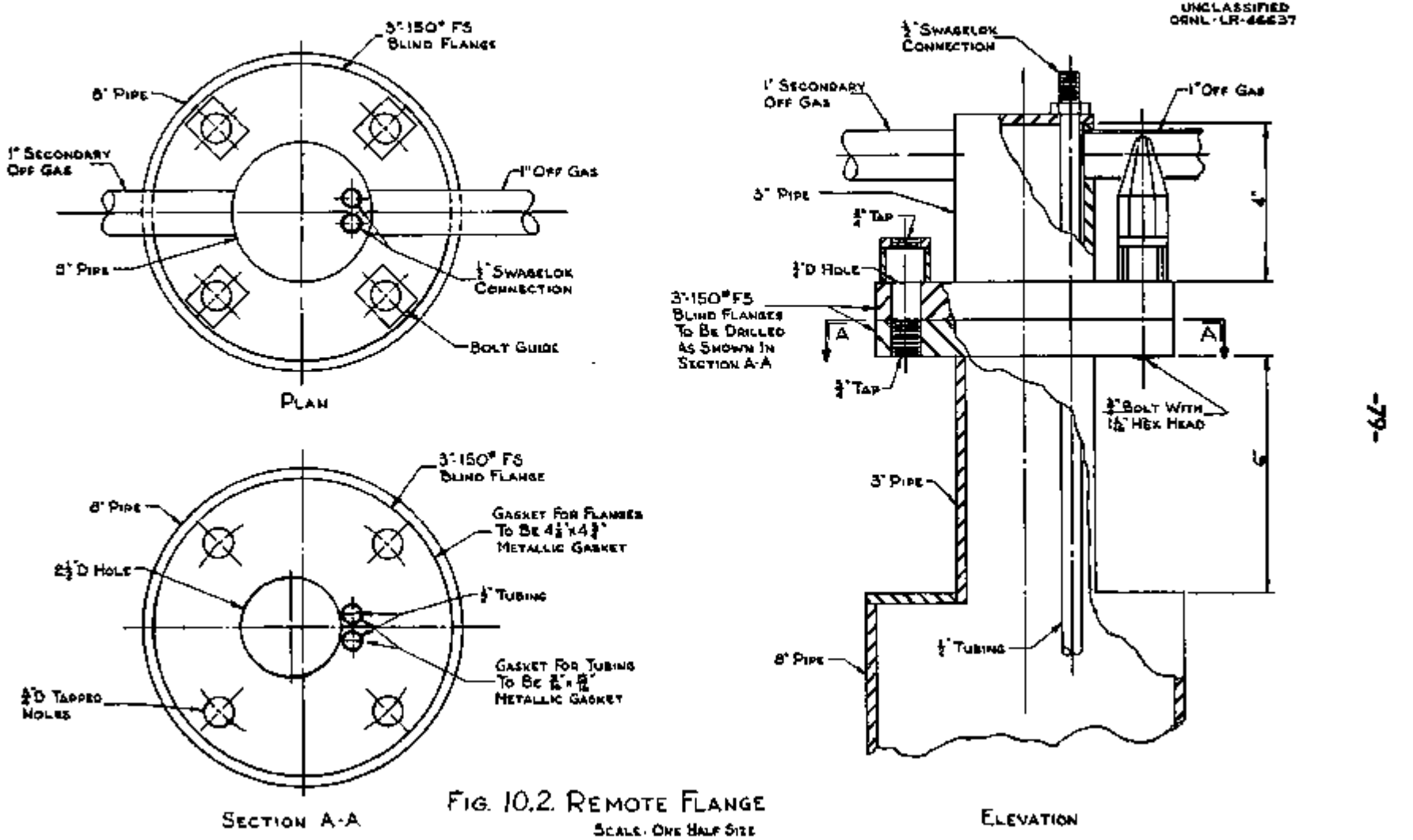

FIG. 10.2. REMOTE FLANGE

SCALE: ONE HALF SIZE

-79-

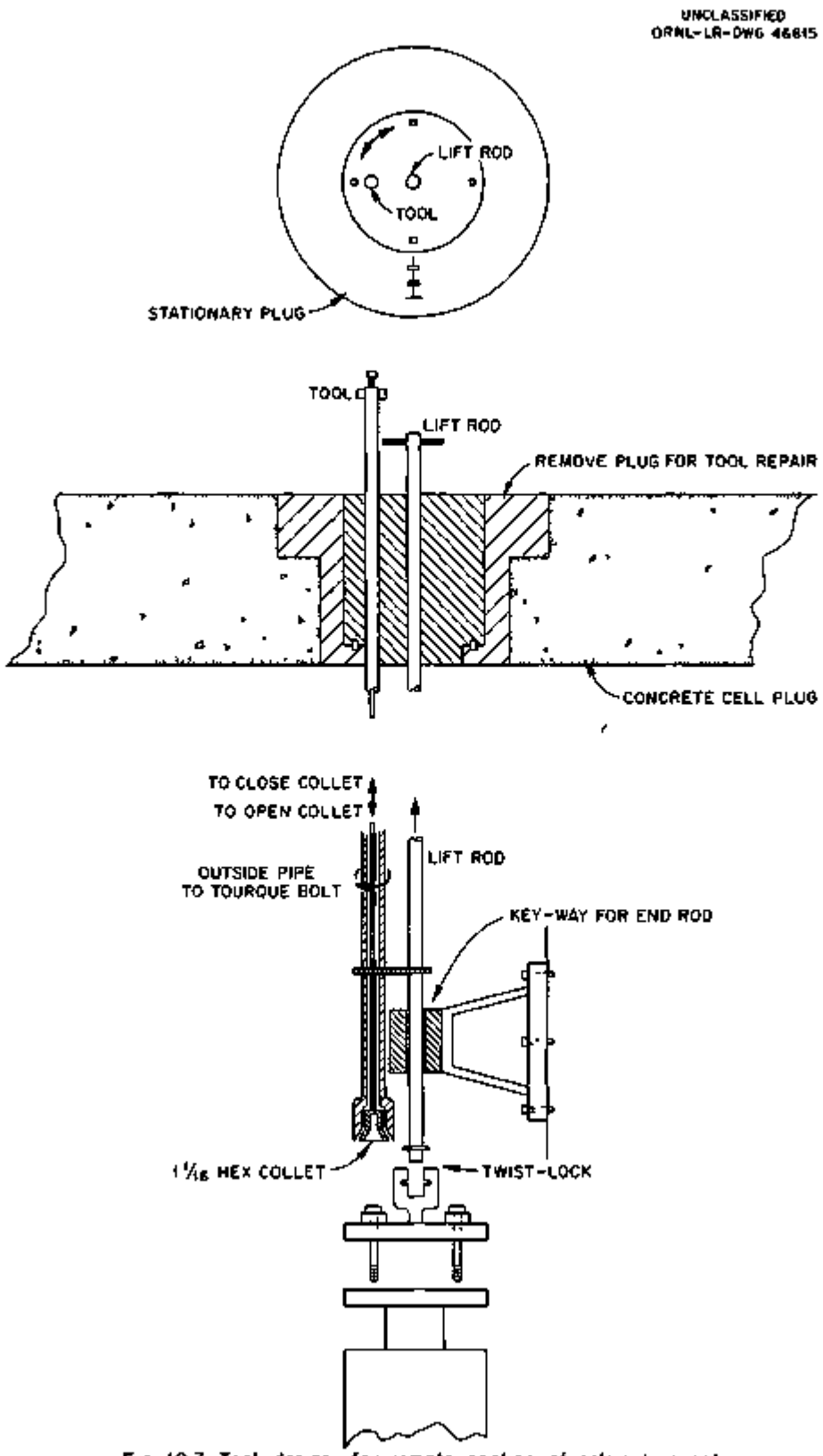

Fig 10 3 Tool design for remote sealing of calcination pot

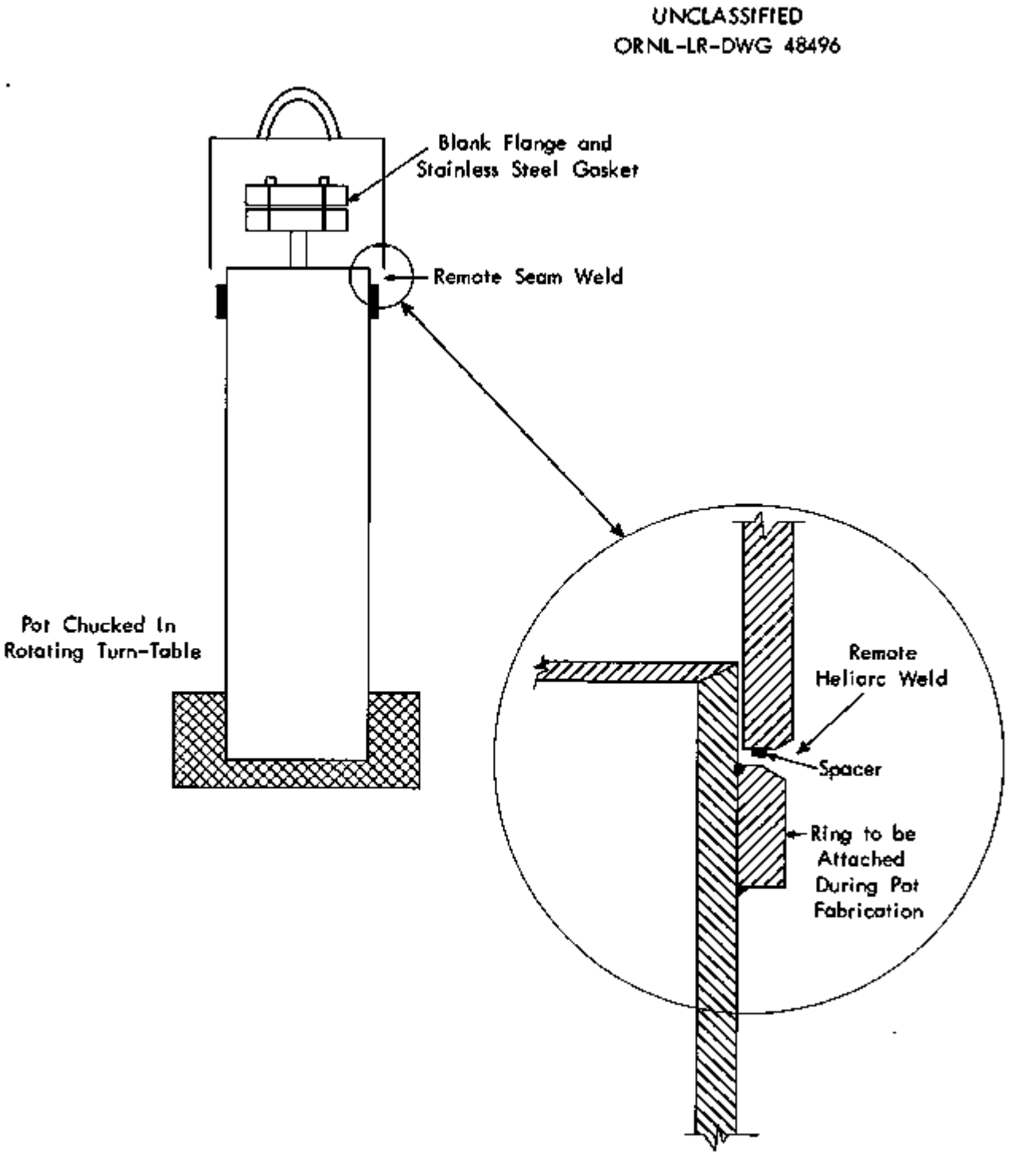

Fig. 10.4. Final seal bonnet for pot calcination.

DISTRIBUTION

1. E. L. Anderson (AEC Washington)
2. F. P. Baranowski (AEC Washington)
3. W. G. Belter (AEC Washington)
4. R. E. Blanco
5. J. O. Blomeke
6. J. C. Bresee
7. R. E. Brooksbank
8. K. B. Brown
9. F. R. Bruce
10. L. P. Bupp (HAPO)
11. W. D. Burch
12. W. H. Carr
13. G. I. Cathers
14. J. T. Christy (HOO)
15. W. E. Clark
16. V. R. Cooper (HAPO)
17. K. E. Cowser
18. F. E. Croxton (Goodyear Atomic Corp.)
19. F. L. Culler, Jr.
20. W. Davis, Jr.
21. O. C. Dean
22. W. K. Eister
23. D. E. Ferguson
24. L. M. Ferris
25. R. J. Flanary
26. E. R. Gilliland (Consultant MIT)
27. H. E. Goeller
28. M. J. Googin (Y-12)
29. A. T. Gresky
30. P. A. Haas
31. M. K. Harmon (HAPO)
32. F. E. Harrington
33. L. P. Hatch (BNL)
34. O. F. Hill (HAPO)
35. J. M. Holmes
36. R. W. Horton
37. A. R. Irvine
38. G. Jasny (Y-12)
39. H. F. Johnson
40. W. H. Jordan
41. S. H. Jury
42. K. K. Kennedy (IDO)
43. L. J. King
44. B. B. Klima
45. E. Lamb
46. D. M. Lang (ORGDP)
47. S. Lawroski (ANL)
48. R. E. Leuze
49. W. H. Lewis
50. J. A. Lieberman (AEC Washington)
51. R. B. Lindauer
52. A. P. Litman
53. J. T. Long
54. B. Manowitz (BNL)
55. J. L. Matherne
56. J. A. McBride (ICPP)
57. J. P. McBride
58. W. T. McDuffee
59. R. A. McNees
60. R. P. Milford
61. J. W. Morris (SRP)
62. D. M. Paige (ICPP)
63. J. R. Parrott
64. F. S. Patton, Jr. (Y-12)
65. Harry Pearlman (AI)
66. R. H. Rainey
67. J. T. Roberts
68. C. A. Rohrmann (HAPO)
69. O. T. Roth (AEC Washington)
70. A. D. Ryon
71. W. F. Schaffer
72. C. H. Secoy
73-75. E. M. Shank
76. M. J. Skinner
77. C. M. Slansky (ICPP)
78. S. H. Smiley (ORGDP)
79. E. G. Struxness
80. J. C. Suddath
81. J. A. Swartout
82. R. J. Teitel (Dow Chemical Co., Midland Mich.)
83. F. M. Tench (Y-12)
84. V. R. Thayer (duPont, Wilmington, Del.)
85. W. E. Unger
86. J. Vanderryn (AEC ORO)
87. F. M. Warzel (ICPP)
88. C. D. Watson
89-118. M. E. Whatley
119. G. C. Williams
120. R. H. Winget
121. C. E. Winters
122. R. G. Wymer
123-124. Central Research Library
125-136. Laboratory Records
137. Laboratory Records (RC)
138. Document Reference Section